



Full-scale trials in heating and combined heat and power plants

Susanne Paulrud, RISE Research institute of Sweden
Nils Skoglund, Umeå University, Sweden

Report :Final REFAWOOD report for WP3-case Sweden

Full-scale trials in heating and combined heat and power plants

Susanne Paulrud, RISE Research institute of Sweden
Nils Skoglund, Umeå University, Sweden

Content

Content	2
Foreword	3
Summary	4
1 Introduction.....	5
2 Full-scale trials with waste wood and gypsum powder as additive in a large-scale CHP in Sweden	5
2.1 Introduction and objectives	5
2.2 Methodology	6
2.1 Determination of gypsum additive levels	6
2.1.1 Stoichiometric approach supported by thermodynamic equilibrium	6
2.2 Full scale combustion tests	9
2.2.1 Description of the plant	9
2.2.2 Production of gypsum additive	10
2.3 Production of fuel mix with additive on terminal	11
2.4 Combustion tests	13
2.4.1 Experimental plan	13
2.4.2 Sampling emissions, particles and deposits.....	13
2.4.3 Chemical analysis by X-ray fluorescence	14
2.4.4 Measuring points.....	14
2.4.5 Fuel, bottom and fly ash samples	14
2.5 SEM-EDS and PXRD analysis	15
3 Results	16
3.1 Fuel blending	16
3.2 Flue gas composition	18
3.3 Ash characteristics	18
3.3.1 Bottom ash.....	18
3.3.2 Fly ash.....	23
3.3.3 Total dust filters	28
3.3.4 Deposition probe	32
3.4 Discussion and conclusions	40
3.4.1 Conclusions	41

Foreword

The work was carried out within the ERA-Net Bioenergy project “REFAWOOD - Resource-efficient fuel additives for reducing ash related operational problems in waste wood combustion” and has been coordinated by RISE Research Institute of Sweden. The project partners consist of six small and medium-sized enterprises and two large companies related to the supply chain of waste biomass power plants and additives, three research organizations and four universities from 5 different countries (Sweden, Austria Germany, Poland and The Netherlands).

This report is part of the deliverables of WP3 Full-scale trials in combined heat and plants.

Summary

Waste wood as demolition wood is today about 10 EUR/MWh cheaper than forest wood chips. However, operation and maintenance-costs (O&M-costs) are higher when this type of waste wood is combusted. The use of additives may reduce the O&M-costs. Therefore, the European Combined heat and power plants (CHP), are highly interested in finding new, low-cost additives to be able to use cheap wood waste without causing an increase in maintenance costs. Within the REFAWOOD project full scale combustion trials have been performed in wood waste fired CHP-plants of different sizes (8-70 MW) and with different technologies.

Within the REFAWOOD project calculated additive levels of gypsum and coal fly ash amounts in the range of 1-3 wt-% for the waste wood fuels used in this work. The additives can be blended with the fuels at a terminal, dosed directly on the fuel at the augers before the furnace or added to the fuel into the boiler by fuel injectors. To be able to adjust the amount, an additive dosing system is preferred. However, the dosing system needs to be adjusted to different fuel feeding systems and to each specific combustion system.

During the full-scale combustion tests the flue gases were analyzed with respect to SO_2 , HCl, NO_x , CO, O_2 , aerosols and total dust particles. When using gypsum as additive, the flue gas analysis shows that the gypsum particles are dehydrated and later decomposes to release gaseous SO_x as shown by the elevated SO_2 levels detected for the cases of gypsum addition. HCl(g) are increased in cases of gypsum addition which further demonstrates that significant amounts of Cl are removed from solid deposits to be found in flue gases instead.

For the gypsum additive, a decrease in the Cl and K-content in the dust can be seen and an increase of the S and Ca-content explained by entrainment of CaSO_4 or CaO from the additive. Common for all measurements is that the chemical composition of the deposits shows that they are mainly comprised by K, Ca, and S which would indicate sulphate formation.

1 Introduction

Today, biomass fuels as different assortments of wood chips, waste and recycled fuels are used at thermal power plants. The use of biomass fuels such as recycled wood fuels can cause troublesome ash-related operational problems, including deposit formation, high temperature corrosion and bed agglomeration in CHP plant facilities. One way to reduce the ash related operational problems is to add additives.

Waste wood as demolition wood is today about 10 EUR/MWh cheaper than forest wood chips. However, operation and maintenance-costs (O&M-costs) are higher when waste wood is combusted. The use of additives may reduce the O&M-costs. Therefore, the European companies (CHP-plants, equipment manufactures) are highly interested in finding new, low-cost additives to be able to use cheap wood waste without causing an increase in maintenance costs.

In WP 3, full scale combustion trials have been performed in four participating countries; Sweden, Poland, Germany and Austria. The trials demonstrate the effect of different resource efficient additives when using wood waste as fuel. The CHP/heating plants in each country have different size, technology, fuelled with different types of wood waste (from demolition wood to low quality forest waste).

The objective of WP3 was to perform full-scale combustion tests to demonstrate effective fuel additive design concepts where the effect of the additive is studied with respect to particle composition of the fine particles (<1 micron), fouling/high temperature corrosion, slagging and emissions (including SO₂ and HCl).

2 Full-scale trials with waste wood and gypsum powder as additive in a large-scale CHP in Sweden

2.1 Introduction and objectives

In Sweden several large-scale combined heat and power plant (CHP) uses recycled wood fuels as demolition wood. The use of such wood fuels can cause troublesome ash-related operational problems, including deposit formation, high temperature corrosion and bed agglomeration in CHP plant facilities. Gypsum has the potential to address issues related to alkali metals and in the case of demolition wood chips, possibly reduce negative effects of Zn and Pb on high-temperature corrosion as well since these elements can be present at elevated levels in waste wood. The sum formula of gypsum is $\text{CaSO}_4 \cdot 1.5\text{H}_2\text{O}$ and upon heating it consumes energy to decompose in two steps. Initially, crystalline water molecules are removed by dehydration and anhydrite (CaSO_4) is formed. At sufficiently elevated temperatures and depending on the surrounding atmosphere this compound decomposes further into CaO(s) and $\text{SO}_3\text{(g)}$.

CaO(s) is generally considered to reduce slagging issues in biomass combustion by increasing melting points of silicates, where formation of low-temperature melting alkali silicates is a well-known problem. SO₃(g) adds acidic components in the flue gases which may increase the need for downstream amendments, but sulphur addition is well known to reduce alkali chloride formation in particulate matter. The reduction of chlorides in deposits is positive for the life span of heat exchanger materials. This sulphation may also affect elements such as Zn or Pb that have been suggested to increase the corrosive potential of alkali chlorides in waste wood combustion.

The objective was to perform full-scale combustion tests with a fuel mix containing demolition wood chips and gypsum powder as additives in a biofuel-fired CHP-plant at ENA Energy (55 MW heat, 24 MW electricity) in Sweden.

2.2 Methodology

2.1 Determination of gypsum additive levels

2.1.1 Stoichiometric approach supported by thermodynamic equilibrium

Additive calculations require chemical information about the used fuel feedstock to determine suitable levels. A total of 8 historic demolition wood fuel analyses provided by ENA Energi AB were available and the obtained average composition of ash forming elements is shown in Figure 1. This was used in the stoichiometric approach described in WP1, where the molar ratio of the ash forming elements K, Na, Zn, and Pb, are balanced against total S content in the fuel. Since the S in a fuel blend will only capture volatilized elements if it is released from fuel particles into gas phase and if it undergoes subsequent sulphation reactions. Applying estimated efficiencies of 80% in decomposition and sulphation steps respectively, the stoichiometric additive level for sulphation was calculated at 0.25 wt-% of fuel on dry basis.

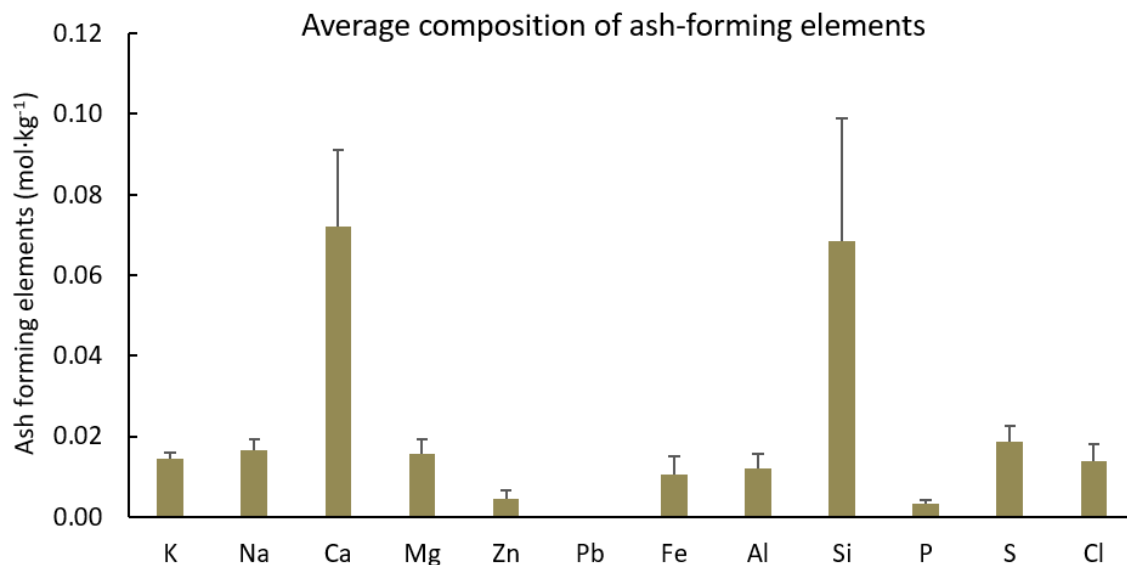


Figure 1. Average ash composition of demolition wood used in calculations presented as fuel fingerprint.

Gypsum addition of only 0.25 wt-% was deemed unsuitable for two reasons. First, the practical aspect of industrial-scale fuel blending with such small additive amounts it improbable that the additive would be readily available for reactions on all parts of the burning fuel bed. Further, the inherent uncertainty in actual additive efficiency makes small additive levels more a theoretical approach than something applicable in industrial settings. For these reasons, it was decided to recalculate for double the stoichiometric amount theoretically required for complete sulphation. This yielded an additive level of 0.85 wt-%, which was further increased to 1 wt-% of gypsum additive on dry basis for practical reasons.

Thermodynamic equilibrium calculations were used to estimate the effect of mixing of additives (gypsum) in a fuel mix of recovered waste wood on the slagging and the deposit forming tendency. The software and databases used were FactSage 7.2 with FactPS, FTOxid, and FTSalt. For simplicity, the total calculations for solid state interactions are provided below to discuss the behaviour of bottom ash. In reality some elements are volatilized during fuel burnout, which removes compounds such as KCl(s) in the bottom ash. The average historic fuel composition was predicted to produce extensive slag formation over 1000 °C (Figure 2), temperatures readily reached in grate-fired systems. With 1% additive in Figure 3, the slag formation was seemingly reduced where the predicted increase between 1060 °C and 1160 °C is likely a by-product of poor data for the phase $\text{Ca}_3\text{Si}_2\text{O}_7$, which disappears and reappears at those changes in slag amount.

The relative stability of $\text{CaSO}_4(\text{s})$ under oxidative conditions is readily seen in Figure 3 as well. The last sulphate predicted by thermodynamics disappears over 1020 °C. Besides this, alkali sulphates such as K_2SO_4 , $\text{K}_3\text{Na}(\text{SO}_4)_2$ and $\text{K}_2\text{CaSO}_4(\text{s})$ are predicted as stable in both cases. The two first are expected products of increased sulphation in the flue gas by gypsum additives, whereas the mixed $\text{K}_2\text{CaSO}_4(\text{s})$ is more likely to appear in the bottom ash as well as in entrained ash fractions.

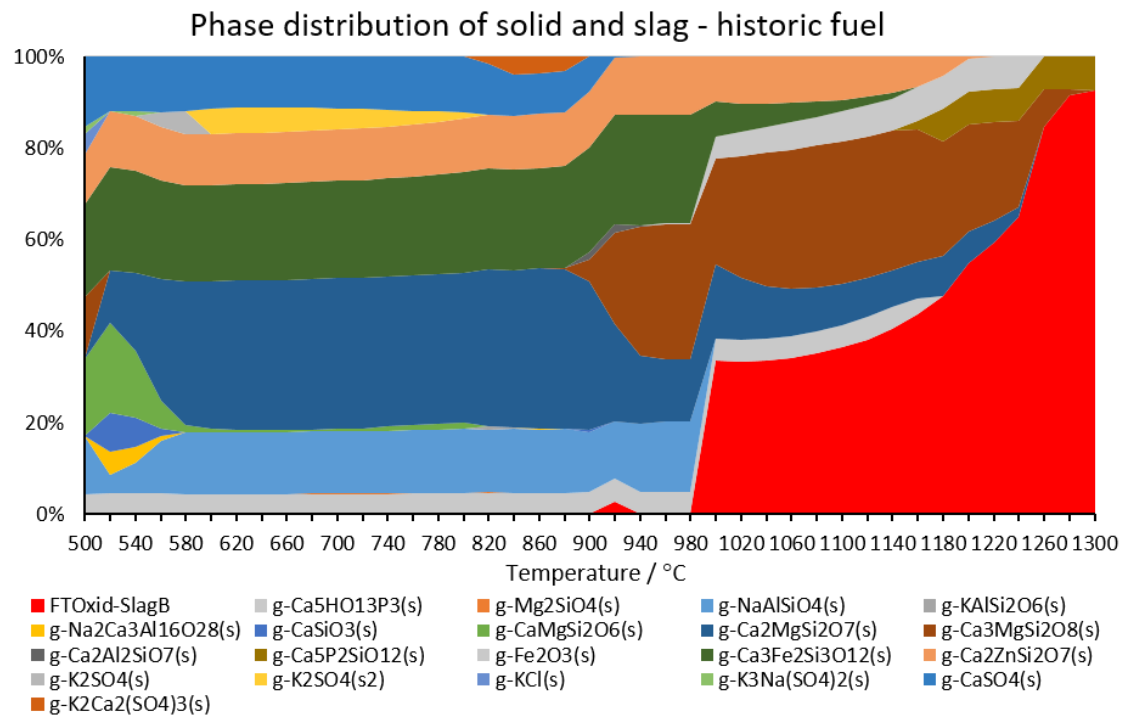


Figure 2. Estimated slag fraction in mass of bottom ash shown in red.

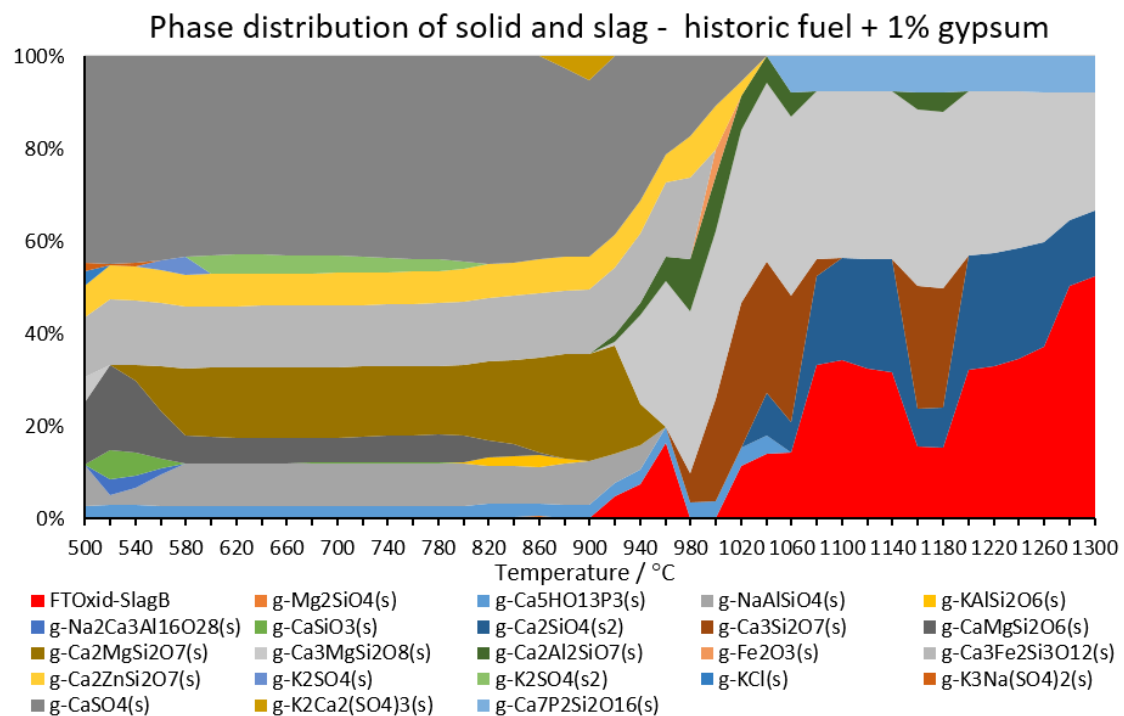


Figure 3. Estimated slag fraction of historic fuel with 1% gypsum additive shown in red. The increase and decrease between 1060 °C and 1160 °C is likely an artefact due to poor stability data in this interval for the compound $\text{Ca}_3\text{Si}_2\text{O}_7(\text{s})$, brown area that mirrors this behavior.

2.2 Full scale combustion tests

2.2.1 Description of the plant

In this task full-scale combustion tests were performed with a fuel mix containing recycled wood chips and gypsum powder as additives in a biofuel-fired CHP-plant at ENA Energy (55 MW heat, 24 MW electricity) in Sweden. ENA Energy AB (ENA) is a municipally-owned limited liability company that was formed in 1972. The company produces electricity and district heating from almost 100 % bio fuel since the middle of the 1990s, which was when the CHP station was put into operation. The district heating is delivered to companies and private households in Enköping.



Figure 4. ENA CHP-plant.

The biomass CHP plant where the combustion tests were performed, consists of a grate boiler built in 1994. The boiler is a Burmeister & Wain with vibration grate. The fuel is thrown into the grate with a spreader. The grate vibrates at regular intervals for fuel and ashes to move forward. Furthermore, the grate tilts to facilitate removal of bottom ash. Primary air is supplied under the grate, as secondary and tertiary air is supplied at different levels in the fireplace above the grate.

Current fuel is 90-100% demolition wood chips. To be able to use 100 % wood waste the furnace is clad with inconel-625 (corrosion- and oxidation-resistant material). The superheaters have gradually been replaced with corrosion-resistant material. Water soot blowers are used to keep the furnace walls clean.

For the purification of nitrogen oxide emissions, a Selective Non Catalytic Reduction (SNCR) system is installed in the boiler. In the SNCR system, ammonia is injected to reduce NO_x . Dust from the combustion process is reduced in an electrostatic filter. SO_2 and HCl are captured in the flue gas condenser, the condensate water from it becomes acidic and neutralized by the addition of lye.

Since the boiler was re-built for wood waste, sulfur has been used as additive to reduce problems with corrosion. The additive is dosed on the augers before the furnace.

The CHP plant has not any experiences of not using sulphur additives since they started to use demolition wood. The purpose to participate in the combustion trials was to test if gypsum could be an option to sulphur additive.

2.2.2 Production of gypsum additive

The gypsum powder was delivered by Gips Recycling AB that is located in Bålsta, 10 km from the fuel terminal. The company converts gypsum waste into recycled gypsum powder to be used by plasterboards manufacturers. The recycled gypsum substitutes virgin or synthetic (FDG or DSG) gypsum as a raw material. At the recycling facility, a mobile recycling units removes all contaminants and the paper backing of the boards, and grinds the gypsum core into clean recycled gypsum powder.



Figure 5. gypsum powder.

Table 1. Chemical composition of gypsum powder.

	Wt-% dm
Cl	0.04
S	21.3
N	0.05
Al	0.30
Si	1.13
Fe	0.12
Ti	<0.1
Mn	<0.1
Mg	0.25
Ca	25.5
Ba	<0.1
Na	<0.1
K	0.31
P	<0.1

2.3 Production of fuel mix with additive on terminal

The wood chips used for the combustion tests were prepared at Ragn-Sells facility in Högbytorp. In addition to demolition wood (impregnated wood is sorted out), the material, also contained smaller amounts of metal, plastic, paper, stone, glass and textile material. Figure 6 shows an image on the recycled waste wood, and the composition of the gypsum is shown in Table 1 above.



Figure 6. Example of recycled waste wood as delivered.

300 tonnes of fuel was prepared for each of the four combustion test. One reference case without additive; two cases where 1% gypsum additive was mixed in two different ways with the fuel; and a fourth case where additive was dosed directly on the fuel at the augers before the furnace. Based on the studies carried out in work package 1, the addition of 1% gypsum was recommended due to losses during preparation.

When preparing fuel mix G1, gypsum and waste wood was first mixed in a pile. The fuel was then lifted to the chip crusher using a gripping claw (Figure 7). For the second fuel mix G2, gypsum was similarly mixed with wood chips and then fed through an Alubucket to achieve a homogeneous mixture (Figure 8).



Figure 7. Fuel admixing (right) and chip crushing (left).



Figure 8. Alu-bucket used in preparation of fuel mixture G2.

2.4 Combustion tests

2.4.1 Experimental plan

Four trials were conducted lasting approximately 24 hours, respectively, of which measurements were carried out during daytime (08:00 to 16:00). During the trials, the same fuel composition was used but the additive was mixed with the fuel in three different ways. G1 and G2 was mixed at the terminal and for G3 the gypsum additive was dosed on the auger before the boiler by using a temporary doser (Figure 9). The doser was adjusted to give the same SO₂ emission level as when sulfur additive was used.

Table 2. Fuel and additive level.

Trial	Fuel	Additive
1	Demolition wood	No additive
2	Demolition wood (Alu-bucket)	1 % Gypsum
3	Demolition wood	1 % Gypsum
4	Demolition wood	Dosing Gypsum



Figure 9. Temporary doser used for the gypsum powder.

2.4.2 Sampling emissions, particles and deposits

The flue gases were analyzed with respect to SO₂, HCl, NO_x, CO, CO₂, and O₂. To determine the particles (mass) size distribution and aerodynamic diameter as well as the chemical composition of each particle fraction size, a low-pressure impactor (LPI)

was used. The particles were divided into 14 size fractions. Total dust samples were taken out in connection with impactor measurements.

During all experiments, the deposit formation was measured on a simulated super heater tube for 4 h. The deposit growth was quantified by a so-called "cold finger", consisting of an air-cooled probe with removable sample rings. The cooled surface temperature of each sample ring was set at 430, 480 and 530 °C and was maintained throughout the test period. The flue gas temperature where the probe was located was around 550 °C.



Figure 10. Deposit probe.

2.4.3 Chemical analysis by X-ray fluorescence

Sampled particle from the impactor and the deposit probe rings were analyzed by chemical composition by X-Ray Fluorescence (XRF). A number of deposit samples were also analyzed by X-Ray Diffraction (XRD) analysis to identify the crystalline phases in the samples.

2.4.4 Measuring points

The measure point for the flue gas analysis, dust analysis and particle analysis were at the end of the superheater. The measure point for the deposit and HCl measurements was before the superheater.

2.4.5 Fuel, bottom and fly ash samples

Fuel samples fly ash samples and bottom ash samples were taken three times during the test period for each trial and a general sample was compiled after each trial. The samples were analyzed according to standard methods of RISE:s fuel accredited laboratory.



Figure 11. Fuel transporter and bottom ash.



Figure 12. Sampling of fly ash.

2.5 SEM-EDS and PXRD analysis

Morphology of the ash fractions was characterized using variable-pressure scanning electron microscopy (VP-SEM; Carl Zeiss Evo LS-15), using a backscattered electron detector at an accelerating voltage of 20 kV and probe current of 500 pA. The elemental composition was quantified using an energy-dispersive X-ray spectrometer (EDS; Oxford Instruments X-Max 80 mm²). These analyses were performed at Umeå Core Facility for Electron Microscopy (UCEM), Chemical Biological Centre (KBC), Umeå University (Umeå, Sweden).

Three replicate samples were used for each original sample. Three replicates were also taken from each filter, there were two filters for each experiment. Area and point analysis were performed from different parts of the samples. An average composition was obtained by calculating the average composition for all three replicate samples and its area analysis. For the bottom ash samples, significant amounts of carbon were present and the analyses could only be performed on and around particles where the ash content was quite high. Because of the heterogeneity of the samples, average values for these samples are indicative between samples. The fly ash samples were generally more homogeneous and allowed for more accurate average elemental compositions.

Due to this heterogeneity of the bottom ash samples and suspicious fractionation of the fly ash samples, ICP analysis of fly- and bottom ash was used instead of the SEM analysis for the bulk evaluation of the samples. This seems more reliable, with a larger amount of sample analyzed.

The amounts of deposit on the deposit probe rings was in some cases really low (especially for the reference case (probe ring nr 4, both sides), gypsum mixture 1 (probe ring nr 7, both sides) and lee side of gypsum mixture 3 (probe ring nr 22)). The low amounts of deposit resulted in high amounts of Fe and Cr, which probably came from the probe rings, when scraping of the deposits.

Powder X-ray diffraction (PXRD) was used to determine which compounds were formed in the bottom ash and fly ash, as several of the other samples provided too little material for accurate analysis. A Bruker d8Advance instrument with Cu-K α radiation, an optical configuration of a 1.0 mm divergence slit and a V α ntec-1 detector was used to collect diffractograms in θ - θ mode and using continuous scans. The initial phase identification was made using Bruker EVA software with the PDF-2 database and the following semi-quantitative analysis using Rietveld refinement was made with structures from ICSD Web.

3 Results

3.1 Fuel blending

The resulting fuel blends from the different blending strategies are shown in Table 3. The inherent variations in fuel composition are indicated by differences between the cases of Ref and G3, since the additive was introduced at the belt conveyor for G3. Ca and Si are present at fairly high concentrations and differ by a factor of almost three between Ref and G3, whereas the alkali metals K and Na only are present at low concentrations but show a similar difference. For the cases with gypsum, G1 and G2, the S-content is notably increased but the concentration of Ca is largely determined by variations in the rest of the fuel. Such inherent variances in fuel composition are a challenge when choosing an additive strategy. In this case the additive levels were over twice the theoretical amounts from a stoichiometric point of view which helps mitigate issues with such variation in very inhomogeneous fuel compositions.

Table 3 Fuel analysis of resulting fuel mixtures of the different additive strategies.

Fuel	Ref	G1	G2	G3
Moister, w-%	19	22	24	25
Heating valueMJ/kg ts	18.6	18.3	18.6	18.8
Ash, w-% dm	2.4	3.7	2.1	1.8
Cl w-% dm	0.03	0.05	0.04	0.03
S w-% dm	0.05	0.13	0.10	0.04
C w-% dm	50	49	50	50
H w-% dm	6.1	6.0	6.1	6.1
N w-% dm	0.66	0.95	0.96	0.71
Al w-% dm	0.08	0.22	0.04	0.04
Si w-% dm	0.38	0.72	0.12	0.14
Fe w-% dm	0.04	0.16	0.02	0.03
Ti w-% dm	0.05	0.10	0.03	0.03
Mn w-% dm	0.008	0.01	0.004	0.004
Mg w-% dm	0.04	0.07	0.02	0.02
Ca w-% dm	0.32	0.43	0.16	0.11
Ba w-% dm	0.008	0.012	0.006	0.004
Na w-% dm	0.09	0.07	0.03	0.03
K w-% dm	0.09	0.11	0.03	0.03
P w-% dm	0.006	0.011	0.004	0.003

3.2 Flue gas composition

SO₂ increases markedly when adding gypsum powder as additive. The sharp increase indicates that the addition of additives was somewhat oversized since the blending of additives in the fuel mix succeeded very well. In the third trial where the gypsum was dosed the SO₂ was lower. HCl increased when adding gypsum additive. The Power was slightly higher for Gypsum 2 and 3 as well as the NO_x level.

Table 4. Mean values for the measured gas concentrations in the polluted flue gas. Measure point is end of the superheater.

	O ₂ %	CO ₂ %	CO mg/Nm ³ 6 % O ₂	NO _x mg/Nm ³ 6 % O ₂	SO ₂ mg/Nm ³ 6 % O ₂	HCl mg/Nm ³ 6 % O ₂	Fluegas temp °C	Power MW
Ref	6,1	14,3	43	56	96	15	395	38
Gypsum 1	4,9	15,3	25	73	345	33	432	43
Gypsum 2	4,4	15,7	45	112	358	36	451	52
Gypsum 3	5,8	14,3	34	112	134	31	425	47

3.3 Ash characteristics

3.3.1 Bottom ash

3.3.1.1 Elemental composition

In table 5 the elemental composition of the bottom ash is shown. The composition is quite similar for all elements except for the S-content that increased when gypsum additives were used. Also, the Cl-content increased.

Table 5. Bottom ash composition according to ICP analysis.

Bottom ash	Ref	G1	G2	G3
Cl w-% dm	0.04	0.14	0.11	0.04
S w-% dm	0.44	1.9	1.3	0.52
Al w-% dm	5.2	3.3	3.3	5.1
Si w-% dm	21	12	13	22
Fe w-% dm	3.0	1.9	2.1	2.6
Ti w-% dm	2.5	1.6	1.6	1.8
Mn w-% dm	0.24	0.17	0.16	0.20
Mg w-% dm	1.4	1.0	0.97	1.3
Ca w-% dm	8.4	8.3	7.3	8.4
Ba w-% dm	0.33	0.22	0.20	0.27
Na w-% dm	2.6	1.4	1.6	2.2
K w-% dm	2.2	1.6	1.7	2.3
P w-% dm	0.18	0.14	0.13	0.17
As mg/kg dm	92	159	82	108
Cd mg/kg dm	<1	<1	<1	<1
Cr mg/kg dm	310	310	270	300
Cu mg/kg dm	3000	1600	970	2000
Ni mg/kg dm	75	67	53	74
Pb mg/kg dm	520	330	200	400
Zn mg/kg dm	3600	2900	3100	4400

3.3.1.2 SEM-EDS analysis

The bottom ash samples were very heterogeneous with noticeable amounts of unburned fuel particles readily identified as elongated dark particles in figure 13 for all fuels. The samples analysed with SEM-EDS displayed no signs of slagging issues. Bottom ash particles were mostly evenly distributed as discrete particles with jagged edges. Some particles that appeared to have contained melts, indicated by rounded shapes and inclusion of more or less rounded bubbles. This heterogeneity shows that solid particle interaction through melt formation did not occur to any larger extent for the reference case or any additive cases.

The reference experiment displayed very little S left in the bottom ash. Separate bottom ash particles with K also contained Ca, Al, and Si (Figure 13), suggesting their capture in

high-temperature melting aluminosilicates. For the runs with gypsum mixture 1 and 2, S was found in the bottom ash, also seen in particles during SEM-EDS analysis. Particles with a lot of Ca and S was found for both gypsum mixture G1 and G2 (figure 15, number 2 and figure 16, number 5), indicating that some gypsum probably not have been decomposed. Especially for mixtures G1 and G2, there were also some particles with a lot of S, K and Ca (figure 15, number 4 and figure 16, number 2), indicating that S from the additive have had the intended effect to bond in K. In addition there were also particles consisting of a lot of S and K. The bottom ash from Gypsum mixture 3 show a few particles with a lot of Ca and S figure 18), indicating that it might be some unreacted gypsum particles, but significantly less than for the other samples with gypsum additive. The relative amount of S in the bottom ash was low for this mixture (figure 18).

A distinct difference in elemental composition of bottom ash depending on analysis method was observed, see figure 19. The trends in elemental concentrations of S according to SEM is that there is a higher S concentration for G1, whereas G2 and G3 do not differ that much. The large difference in particle composition shows for SEM-EDS results with quite large error bars for the different elements. SEM-EDS analysis generally display higher Ca and S contents whereas Al and Si concentrations were lower than found in Table 5. This could be related to sample interaction differences between the two analysis methods where SEM-EDS should be considered a surface analysis technique, and could therefore underrepresent elements in thicker particles if they do not have a homogeneous composition.

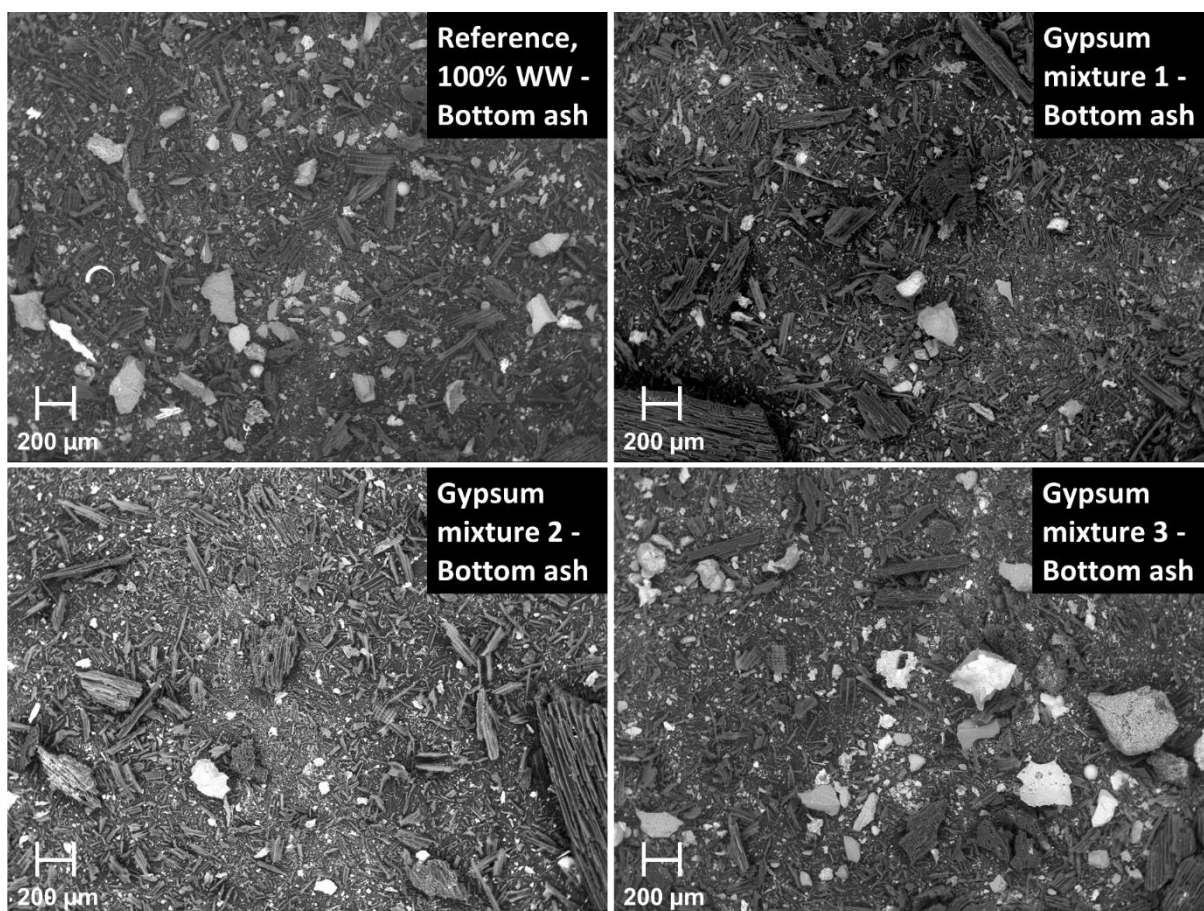


Figure 13. Overview of the bottom ash samples which shows significant amount of fuel particles having undergone partial conversion (dark particles) and different kinds of ash particles.

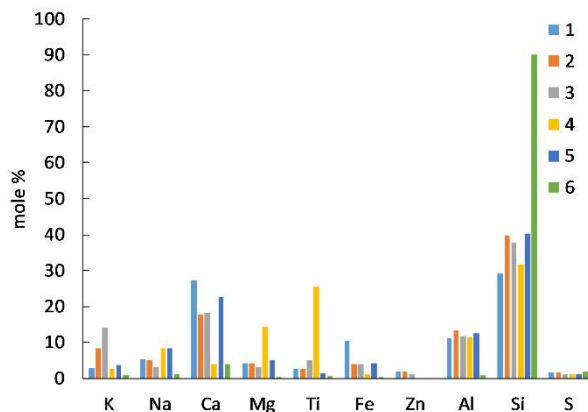
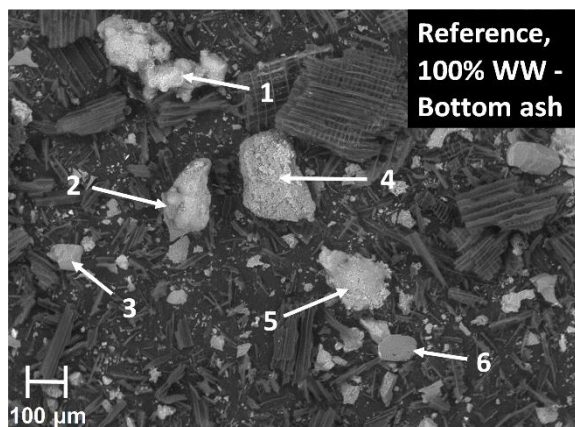


Figure 14. Example of different kinds of particles for bottom ash from the reference run.

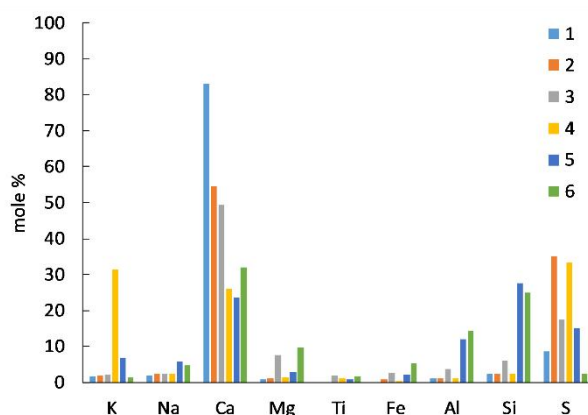


Figure 15. Example of different kinds of particles in the bottom ash from the gypsum mixture 1. Number 2 in the image, with a lot of S and Ca might be a gypsum particle that has not been decomposed. Number 4 is an example where probably the gypsum has reacted with K.

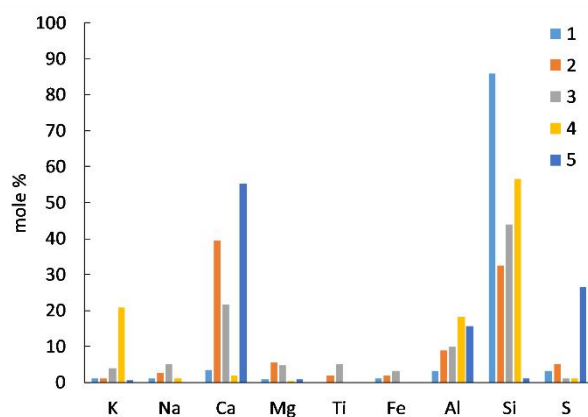
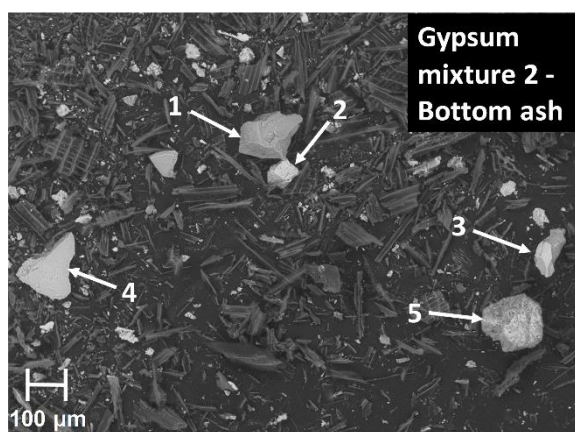


Figure 16. Bottom ash sample from gypsum mixture 2. Example of probably a gypsum particle, number 5 in the image.

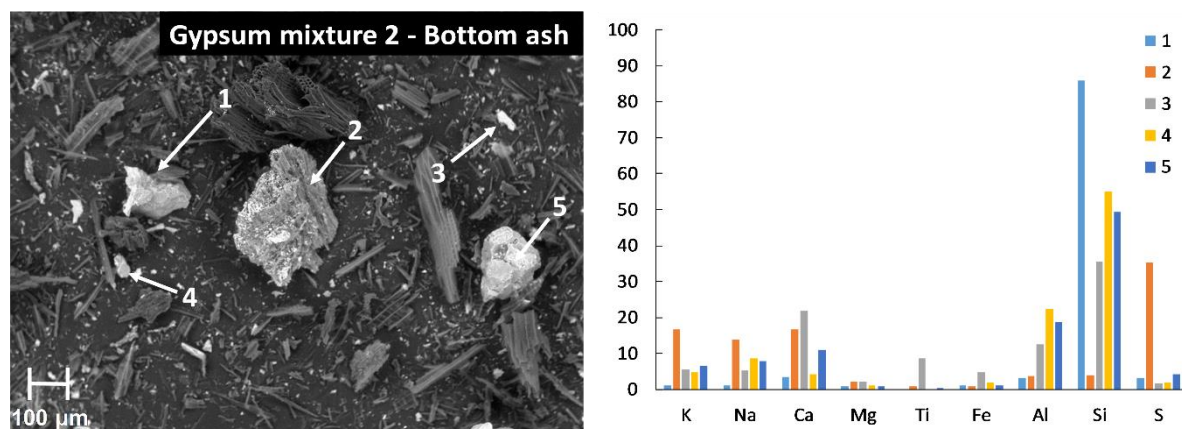


Figure 17. Bottom ash sample from gypsum mixture 2. Example of a particle rich in S, K, Ca and Na in the middle of the image (number 2).

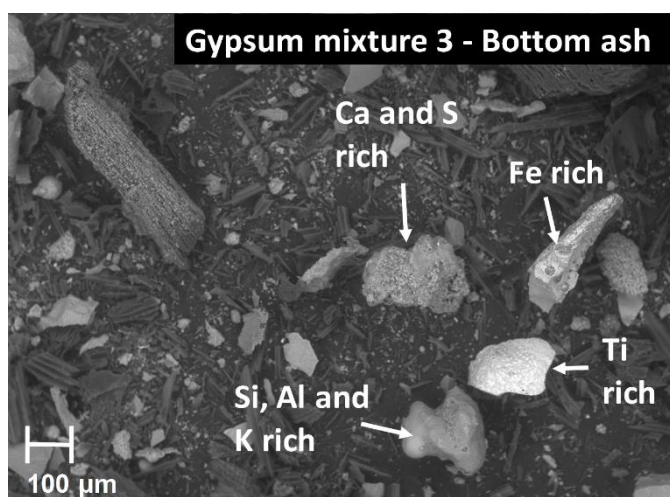


Figure 18. Bottom ash sample from gypsum mixture 3. Example of a Ca and S rich particle that might be a gypsum particle in the middle of the image.

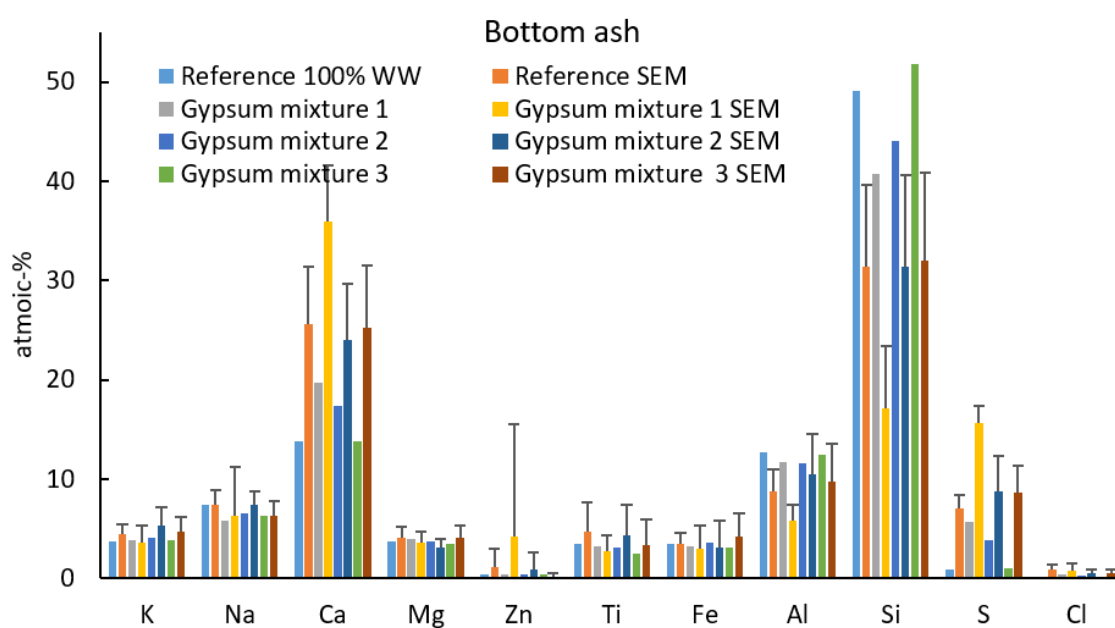


Figure 19. Elemental composition of bottom ash according to SEM-EDS analysis normalized on (C, O)-free basis, compared with XRF results.

3.3.1.3 PXRD-analysis

The results from semi-quantitative analysis provided some additional information concerning the decomposition of gypsum in the fuel bed (Table 6). All cases with additive showed increased formation of calcium sulphate in the bottom ash but the effect on other compounds were less obvious. The presence of sulphates was most notable for the G1 case, probably indicating that some gypsum particles did not fully decompose during fuel conversion. It is however unclear whether these particles are from the original gypsum or have formed due to reaction of gaseous SO_x with CaO on the cooler parts of the grate. G1 and G2, which had the highest gypsum addition, also displayed the highest amount of carbonates identified in the bed. It is likely that at least part of this calcium originates from the introduced gypsum which suggest that the additive did decompose and that the CaO formed is in fact available for subsequent reactions.

Table 6. Semi-quantitative analysis of crystalline content in bottom ashes from industrial-scale experiments presented in wt-% of crystalline material.

Formula	Trivial name	Reference	G1	G2	G3
CaSO ₄	Anhydrite	3	27	13	13
CaCO ₃	Calcite	16	41	35	8
CaMg _{0.75} Al _{0.25} Si ₂ O ₇	Åkermanite	12	9	7	3
NaAlSi ₃ O ₈	Albite	27	5	22	43
SiO ₂	Quartz	34	14	18	24
TiO ₂	Rutile	7	4	6	8
Fe ₂ O ₃	Hematite	2	1	0	1

3.3.2 Fly ash

3.3.2.1 Elemental composition

Fly ash composition was affected similarly for all three additive levels. The Ca, K, Na, Al, and Si levels all increased for G1-G3 compared to the reference. The increase of K and Na in fly ash fractions were very similar. This could possibly be due to surface bonding similar to the K bonded in Ca and S-rich particles found in the bottom ash. While the inhomogeneous fuel has a natural variation in ash-forming elements it is unlikely that this co-variance is coincidental.

Table 7. Fly ash composition according to ICP analysis.

Fly ash	Ref	G1	G2	G3
Cl w-% dm	11.0	10.8	8.7	10.4
S w-% dm	4.4	5.4	4.5	4.2
Al w-% dm	1.5	2.3	2.9	2.9
Si w-% dm	3.9	6.2	8.4	8.3
Fe w-% dm	2.0	2.4	2.7	2.8
Ti w-% dm	1.1	1.7	2.0	2.0
Mn w-% dm	0.22	0.32	0.34	0.36
Mg w-% dm	1.0	1.4	1.7	1.7
Ca w-% dm	6.5	14	15	13
Ba w-% dm	0.17	0.28	0.33	0.32
Na w-% dm	2.1	3.5	3.5	3.8
K w-% dm	1.8	3.5	3.6	3.8
P w-% dm	0.24	0.34	0.39	0.40
As mg/kg dm	2500	2700	1600	2100
Cd mg/kg dm	110	100	77	89
Cr mg/kg dm	370	350	330	350
Cu mg/kg dm	1300	1300	1100	1300
Ni mg/kg dm	98	84	96	98
Pb mg/kg dm	3300	2900	2600	2900
Zn mg/kg dm	48200	46000	41400	43700

3.3.2.2 SEM-EDS analysis

The fly ash has a largely homogeneous appearance with few, smaller particles dispersed in a fine powder for all samples, see Figure 20. Addition of gypsum has effect on overall composition according to SEM-EDS analysis (Figure 21). The difference compared to

values presented in Table 6 probably related to discrete particles with Al and Si. Discernible larger particles were analysed for their elemental composition as shown in Figure 22–Figure 25. There are some distinct chloride particles Single particles with for example a lot of Fe, Ti or Si (and/or Al, Ca, Mg) was found. For the fly ash samples with gypsum additive, there were some diffuse particles that might be small gypsum particles with higher levels of S and Ca. An important observation is that even in single particles rich in Ca and S, their molar ratios are not 1:1. This would be the case if the gypsum additive particles remained as dehydrated gypsum, CaSO_4 , and did not react further.

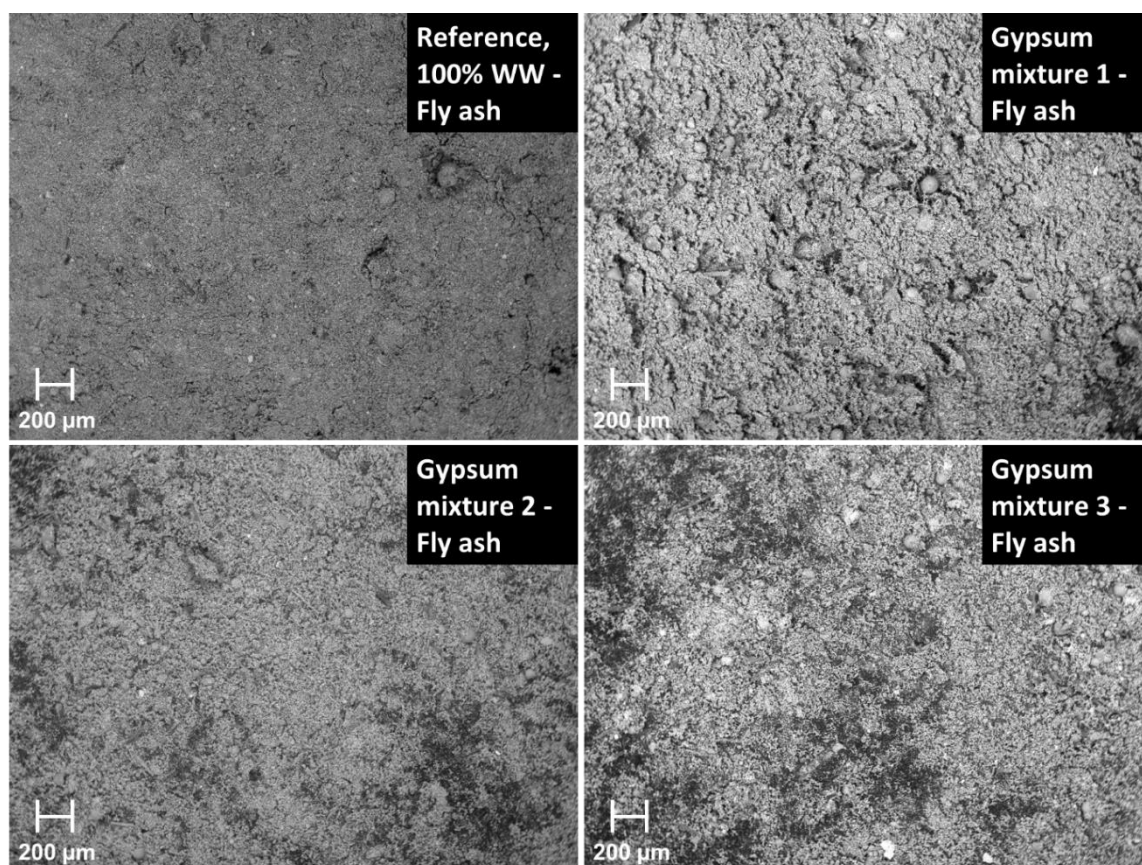


Figure 20. Overview of the fly ash samples.

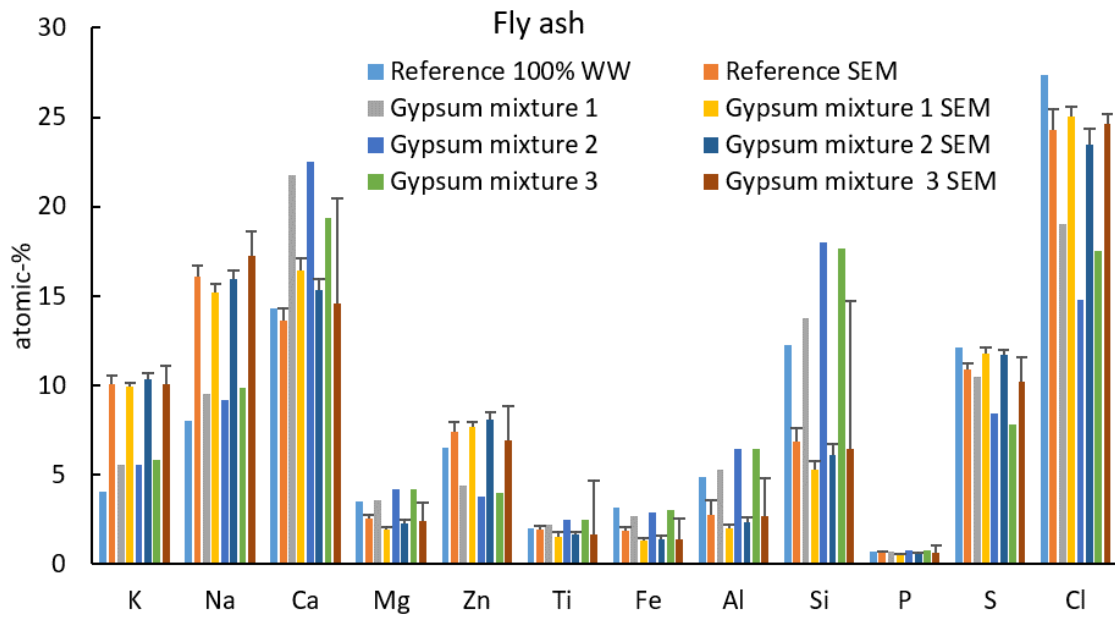


Figure 21. Elemental composition of fly ash according to SEM-EDS analysis normalized on (C, O)-free basis, compared with XRF results.

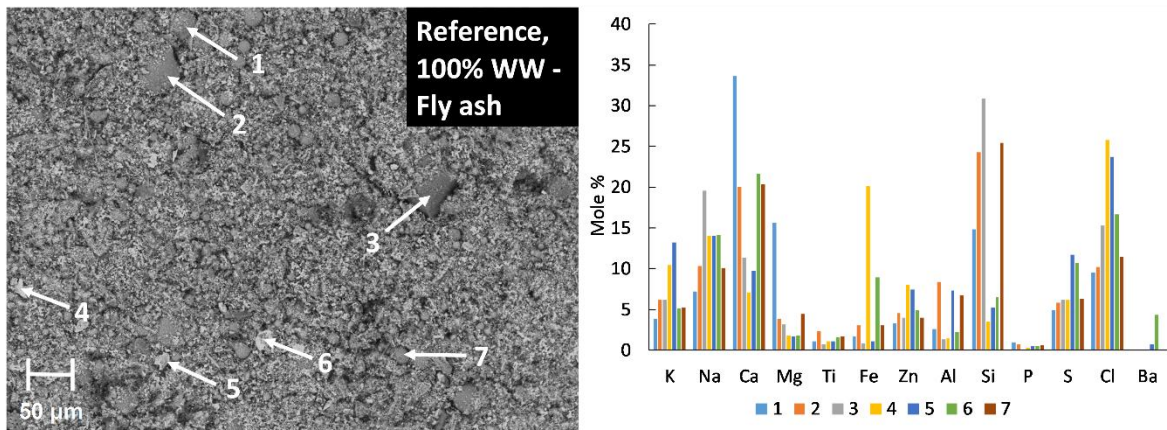


Figure 22. Example of different kinds of particles from the fly ash samples from the reference run.

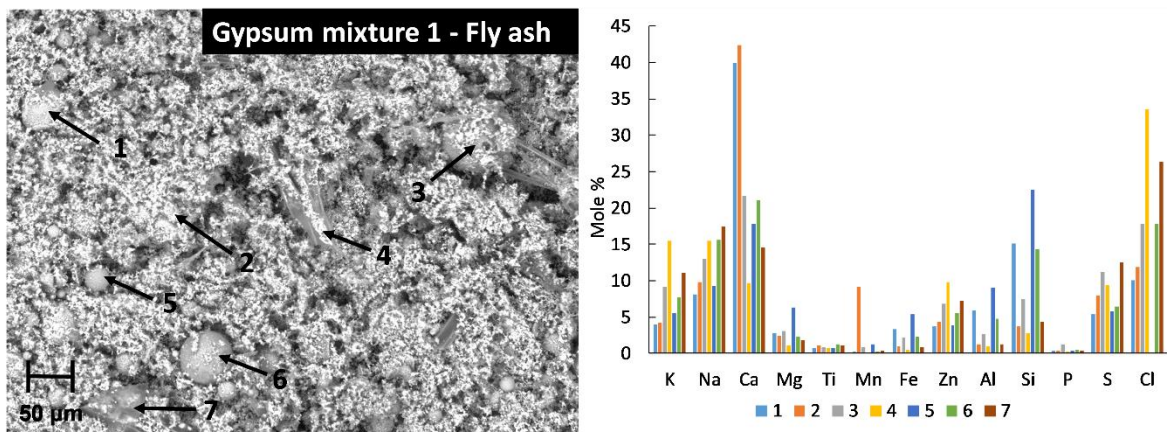


Figure 23. Example of different kinds of particles from the fly ash samples from the run with gypsum mixture 1.

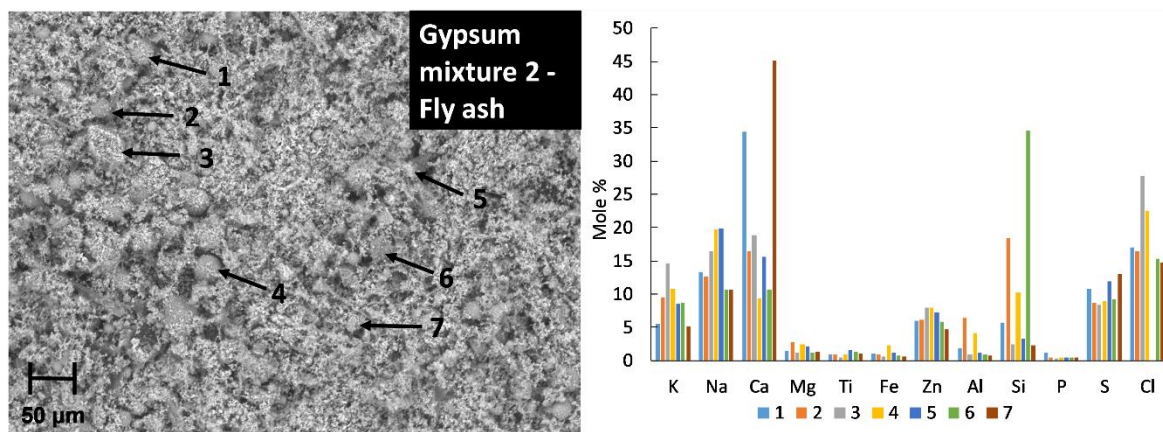


Figure 24. Example of different kinds of particles from the fly ash samples from the run with gypsum mixture 2.

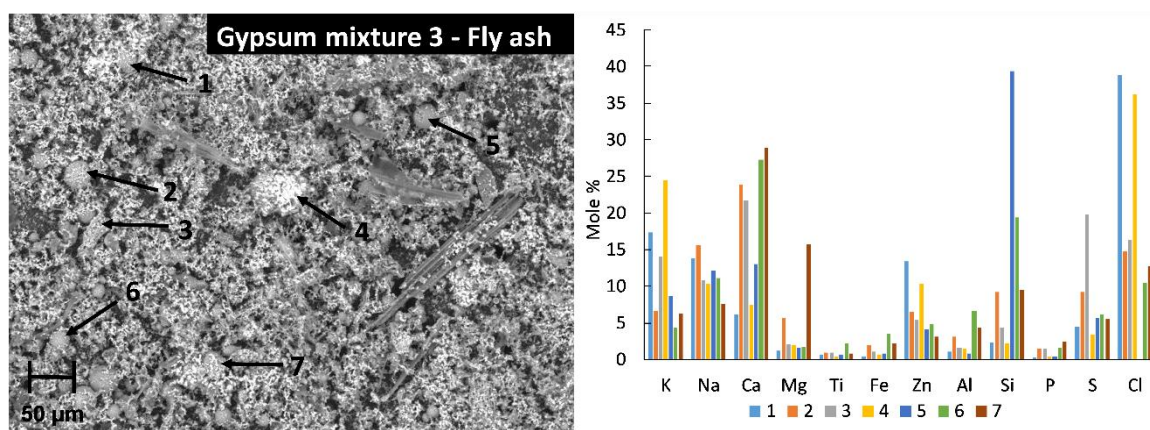


Figure 25. Example of different kinds of particles from the fly ash samples from the run with gypsum mixture 3.

3.3.2.3 PXRD-analysis

Semi-quantitative analysis of crystalline compounds in fly ash show no major differences, see Table 8. This is largely in line with what was observed for the elemental analysis, with potentially some increase in calcium sulphates entrained into the fly ashes. An increase of crystalline CaO is also shown, indicating that some of the calcium from gypsum is entrained into fly ashes as CaO. The main chlorides identified are K_2ZnCl_4 and NaCl, where NaCl may have been affected for cases G1 and G2. No major increase in alkali sulphate formation could be observed in the fly ash.

Table 8. Semi-quantitative analysis of crystalline content in fly ashes from industrial-scale experiments presented in wt-% of crystalline material.

Formula	Trivial name	Reference	G1	G2	G3
CaSO ₄	Anhydrite	18	24	22	21
K ₂ SO ₄	Arkanite	4	5	6	
K ₃ Na(SO ₄) ₂	Aphtitalite	2	2	1	2
NaCl	Halite	13	6	5	12
K ₂ ZnCl ₄		47	47	48	45
CaO	Lime	2	6	6	4
SiO ₂	Quartz	5	4	6	6
MgO	Periclase	4	2	2	4
TiO ₂	Rutile	5	4	4	6
Fe ₂ O ₃	Hematite	1			

3.3.3 Total dust filters

3.3.3.1 Dust load and composition with XRF

The total amount of particulate matter was larger in combustion with gypsum additives as shown in Figure 26. Considering that the gypsum additive level was 1 wt-% of which some is lost as water upon dehydration, this increase is likely not only explained by entrainment of CaSO₄ or CaO from the additive. A decrease in the Cl and K-content can be seen for the highest additive-levels (Figure 27-28) and an increase of the Ca-content (Figure 28).

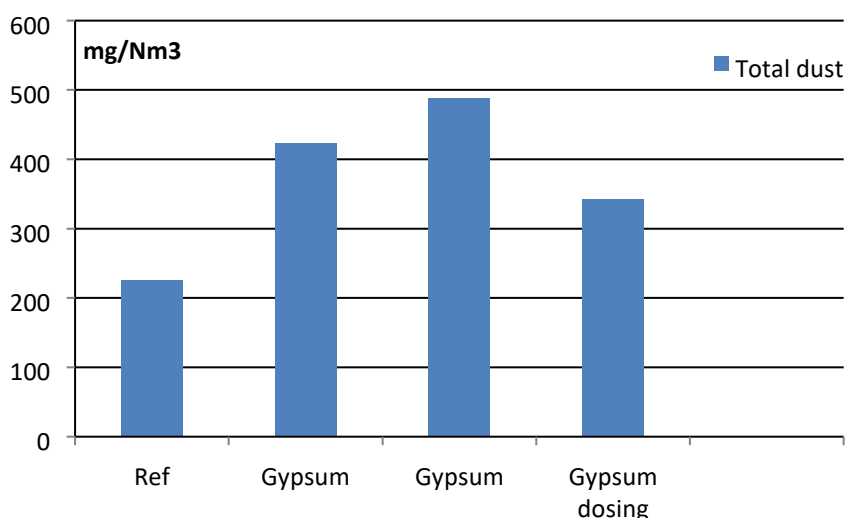


Figure 26. Total dust concentrations normalized to 6% O₂.

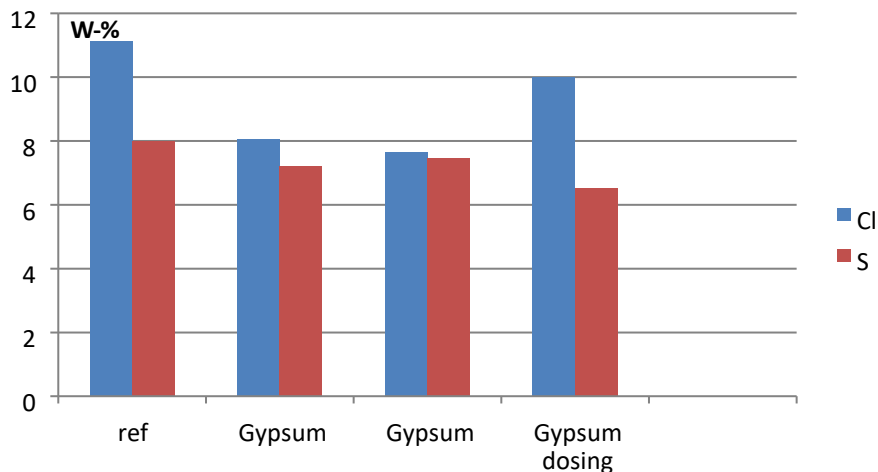


Figure 27. S and Cl concentrations in total dust filters as obtained by XRF analysis.

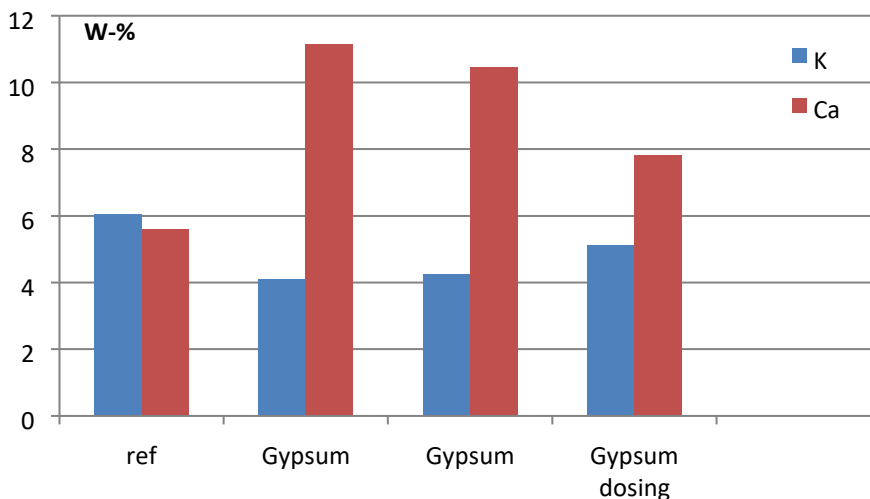


Figure 28. K and Ca concentrations in total dust filters as obtained by XRF analysis.

3.3.3.2 SEM-EDS analysis

The average elemental composition of filter ashes are shown in Figure 29. For additive experiments G1 and G2 there is a clear increase in Ca and S whereas K, Na, and Cl concentrations decrease. Zn levels remain the same for all cases, however. Looking at specific particles from the reference case in Figure30 there is a clear covariance of Na, S, and Cl. K and Zn may be following a similar trend but not as obviously. All experiments with additives displayed at least some particle with similar concentrations of Ca and S, Figure31–Figure36. There are also discrete particles with K and/or Na and Cl that covaries which indicates that alkali chloride formation occurs.

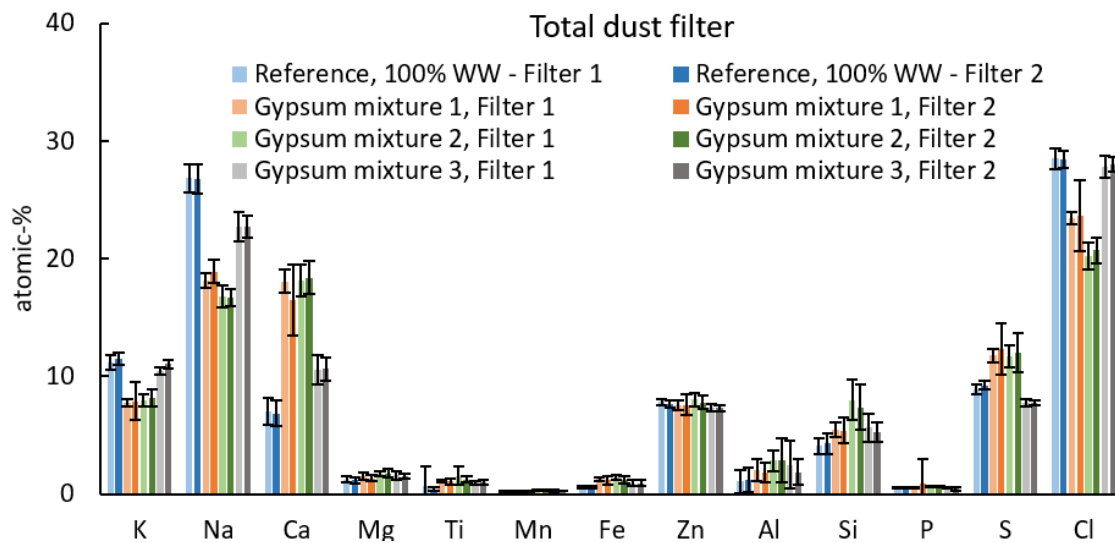


Figure 29. Elemental composition of fly ash according to SEM-EDS analysis normalized on (C, O)-free basis, compared with XRF results.

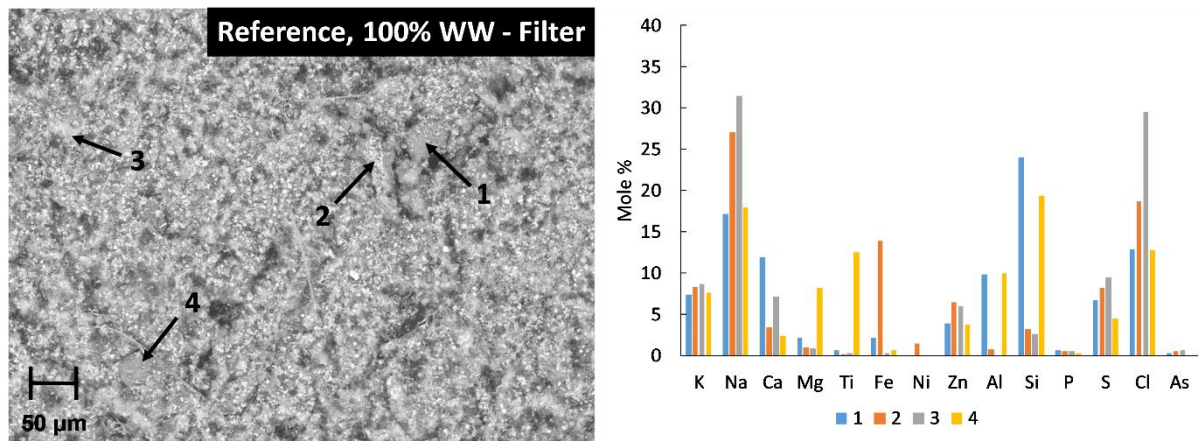


Figure 30. Example of the composition of different particles in the sample from the filter from the reference run.

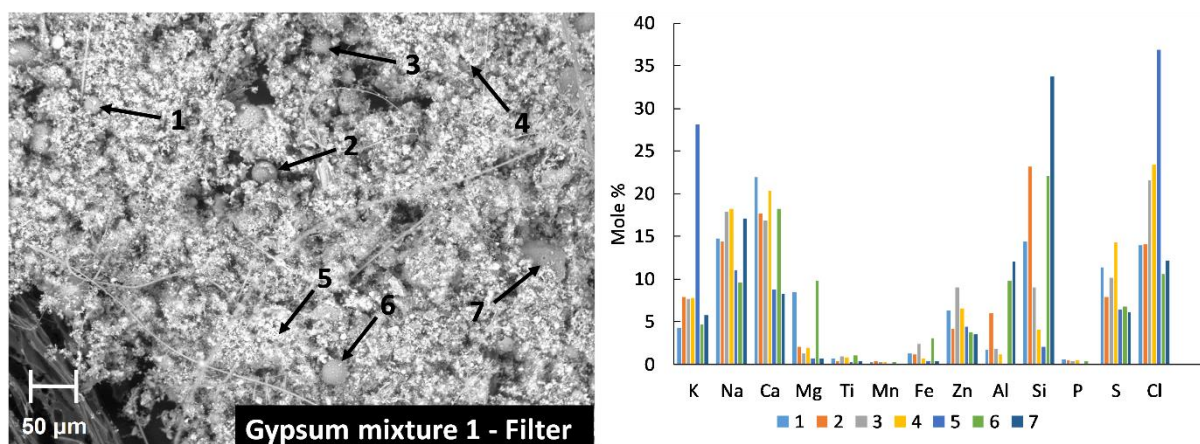


Figure 31. Example of the composition of different particles in the sample from the filter from the run with gypsum mixture 1.

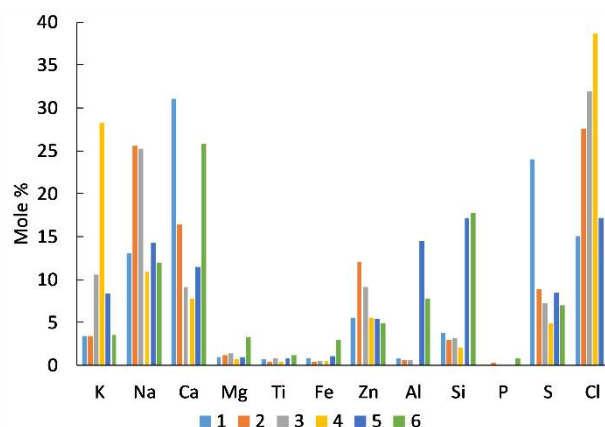
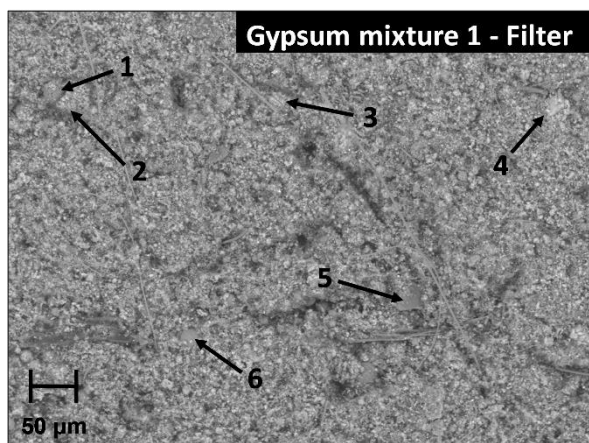


Figure 32. Another example of the composition of different particles in the sample from the filter from the run with gypsum mixture 1. In this view, an example of what might be a small gypsum particle can be found in point number 1 (rich in S and Ca).

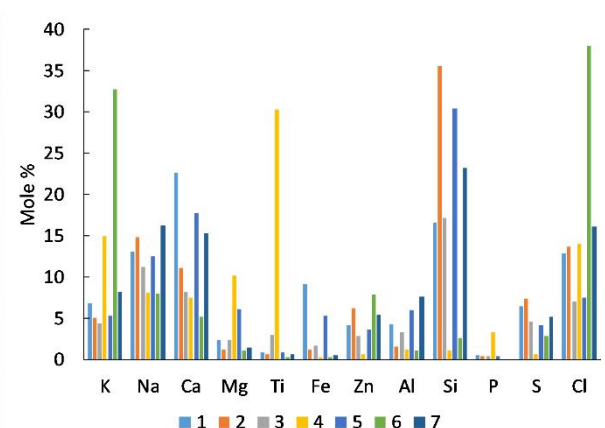
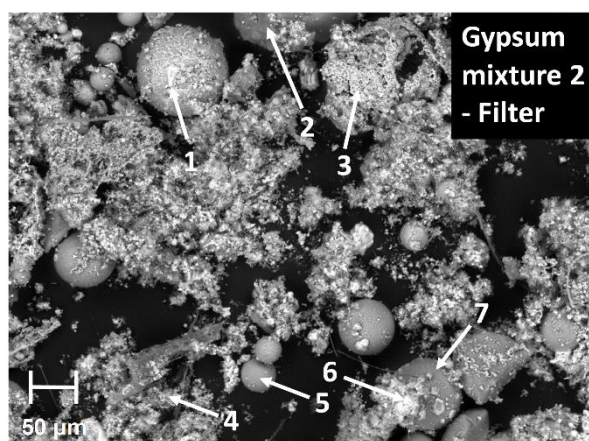


Figure 33. Example of the composition of different particles in the sample from the filter from the run with gypsum mixture 2.

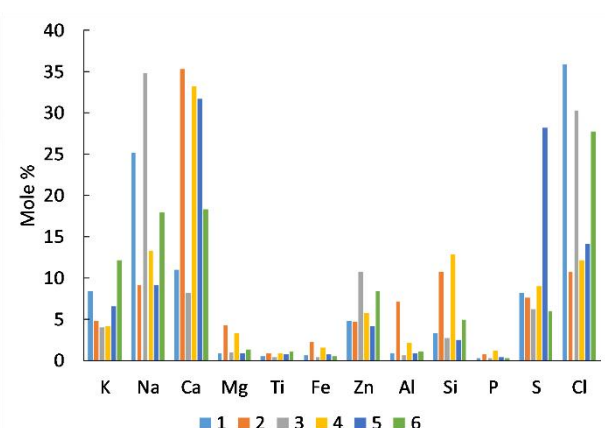
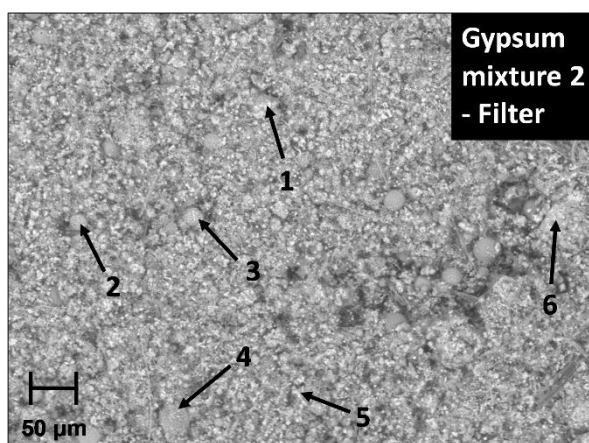


Figure 34. Another example of the composition of different particles in the sample from the filter from the run with gypsum mixture 2. In this view, an example of what might be a small gypsum particle can be found in point number 5 (rich in S and Ca).

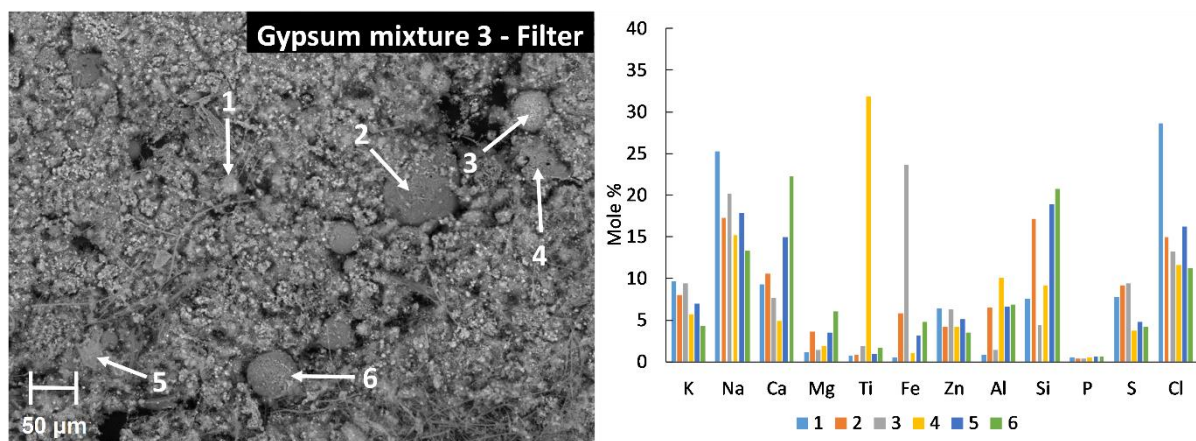


Figure 35. Example of the composition of different particles in the sample from the filter from the run with gypsum mixture 3.

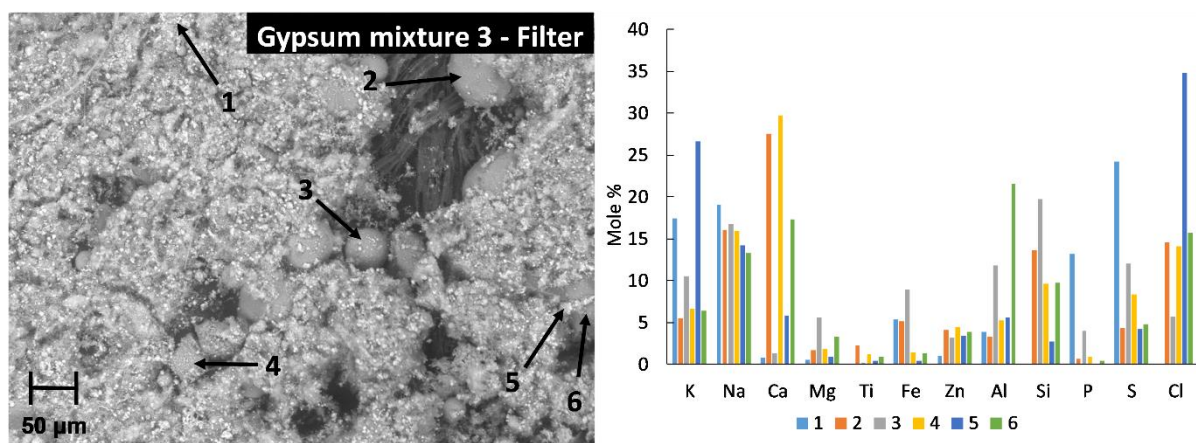


Figure 36. Another example of the composition of different particles in the sample from the filter from the run with gypsum mixture 3.

3.3.4 Deposition probe

3.3.4.1 Deposit growth and chemical composition with XRF

The amount of deposits increased with addition of gypsum, Figure 37. This was most noticeable in the cases of G2 and G3, and the deposit probe with a surface temperature of 525 °C. As shown in the XRF analyses of deposit composition, the main deposits formed are sulphates already for the reference case. Based on this, the potential risk for alkali chloride-induced high-temperature corrosion very small. With gypsum addition this does not change. The increase in deposits is seemingly mainly comprised by K, Ca, and S which would indicate sulphate formation. It is possible that the mode of additive mixing is what made the largest difference between G2 compared to G1 and G3. The Alu-blender may crush part of the additive and fuel into smaller particles than the other additive mixing modes. This does not necessarily mean that it is solely gypsum that is entrained to a larger extent, there could also be a higher presence of fine fuel particles that are more readily entrained for the G2 case.

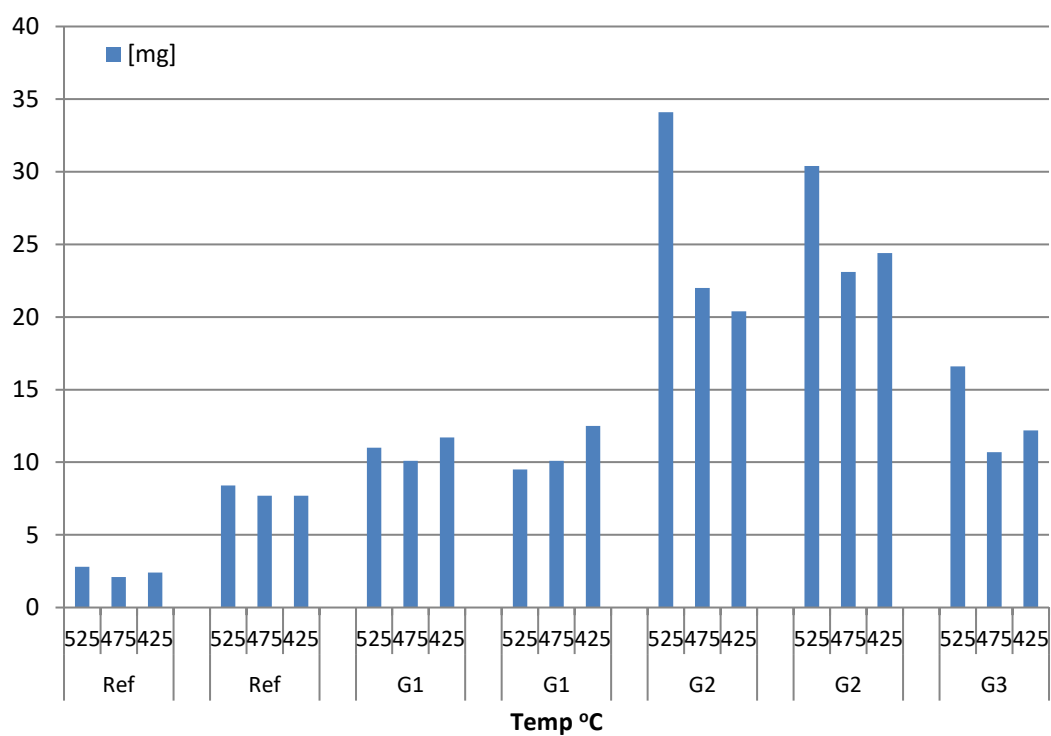


Figure 37. Total amount of deposits on rings with three different temperatures.

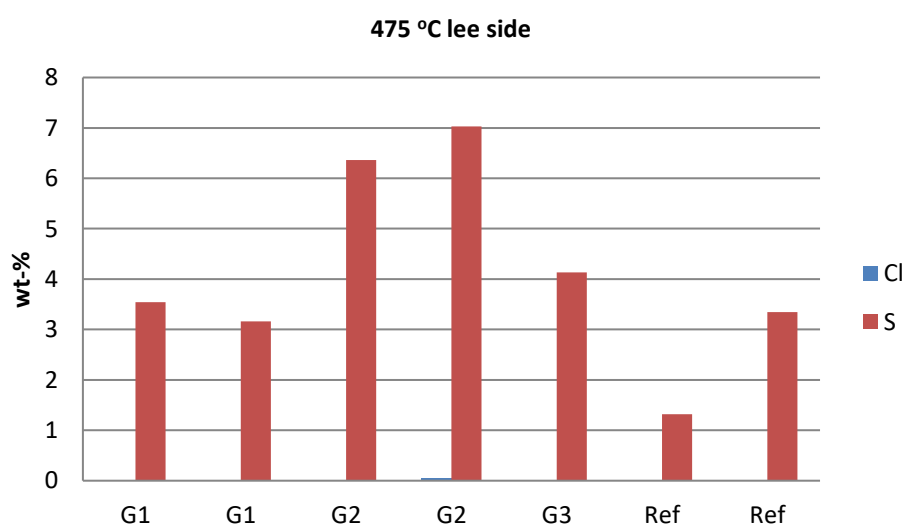


Figure 38. S and Cl concentrations in deposits as obtained by XRF analysis.

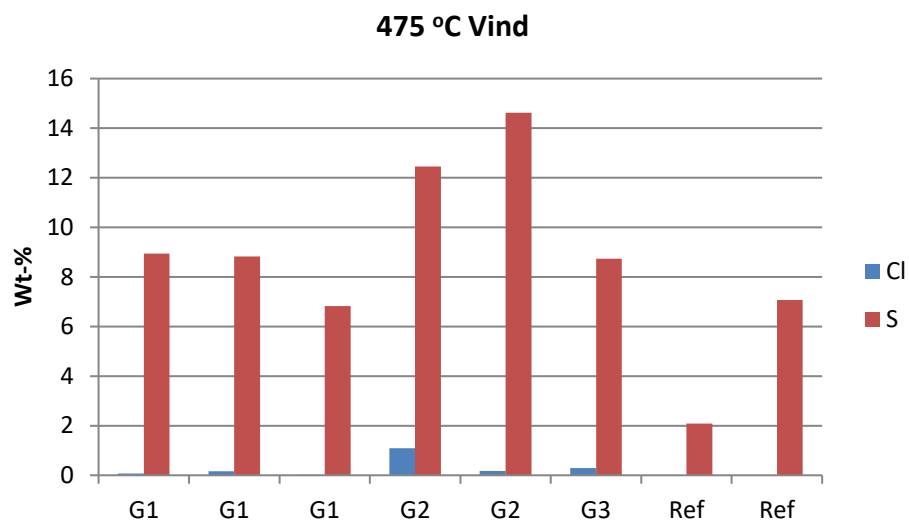


Figure 39. S and Cl concentrations in deposits as obtained by XRF analysis.

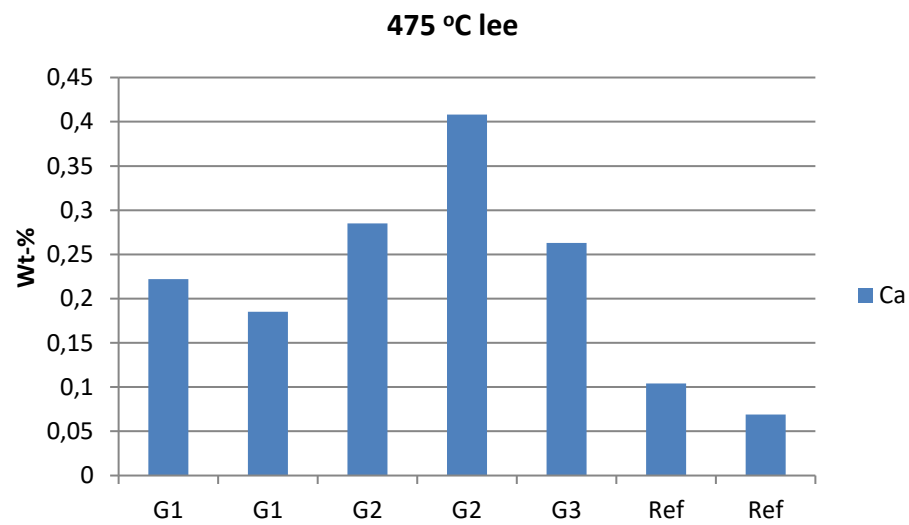


Figure 40. Ca concentrations in deposits as obtained by XRF analysis.

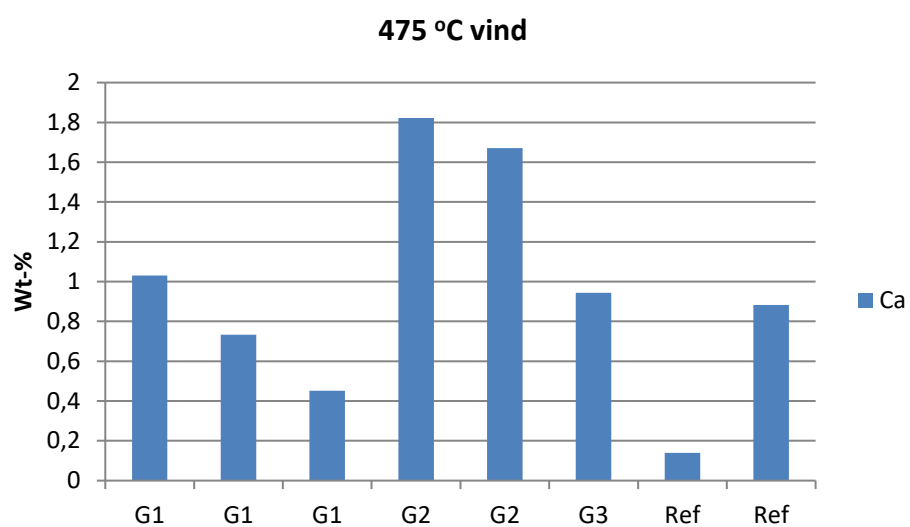


Figure 41. Ca concentrations in deposits as obtained by XRF analysis.

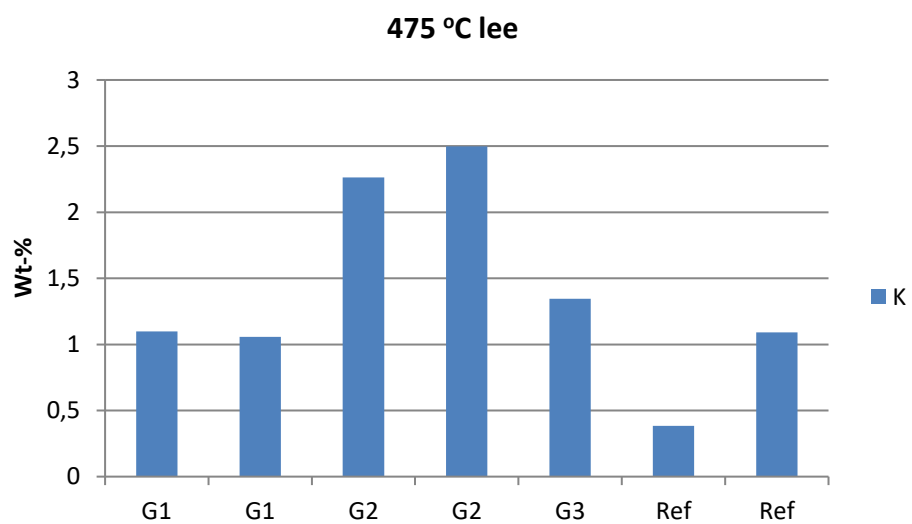


Figure 42. K concentrations in deposits as obtained by XRF analysis.

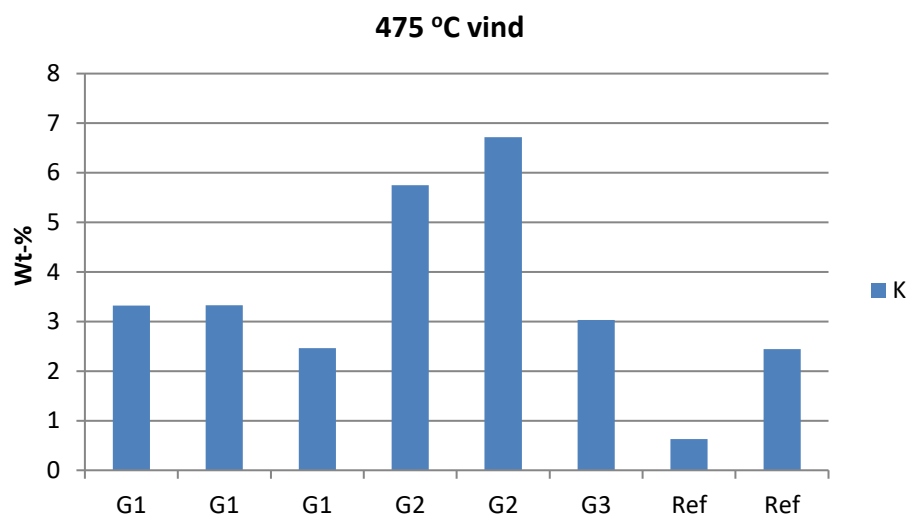


Figure 43. K concentrations in deposits as obtained by XRF analysis.

3.3.4.2 SEM-EDS analysis

The average relative composition of the ash forming elements resulted from SEM-EDS analysis of the deposit probe rings held at 525 °C are shown in Figure 44. The presence of Ca in deposit lee-side with gypsum additives suggest that submicron particles of CaO or CaSO₄ either act as nucleation cores for elements that reacts through gas phase, or are bonded onto an existing deposit. However, only small amounts of deposits were available on the rings, but some discrete particles could be found as shown in Figure 45–52. This could point to that small particles with solid Ca contribute in the formation of fine particulate matter.

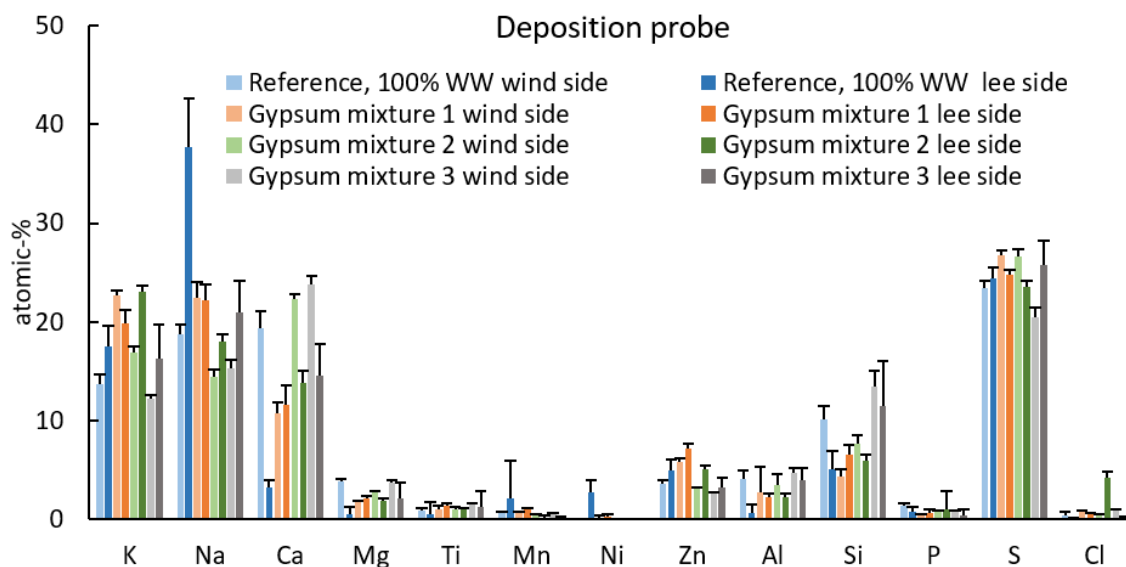


Figure 44. The average relative composition of the ash forming elements for the deposit probe rings, without Fe and Cr and given in O and C free basis. Standard deviation showing the deviations between the average of the sites/areas as error bars.

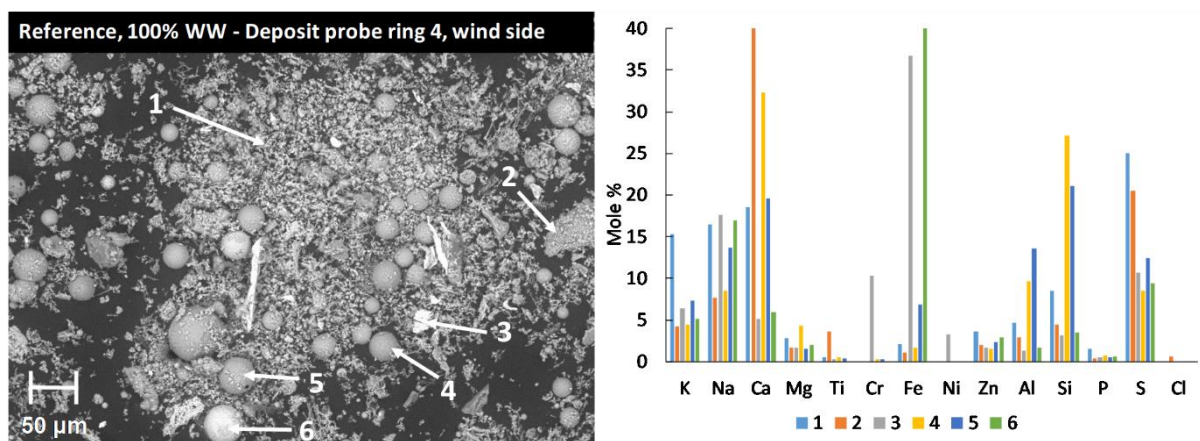


Figure 45. Example of the composition of different particles in the sample from the deposit probe ring, wind side, from the reference run. Here, the Fe and Cr rich, light particle (nr 3), probably has originated from the probe rings.

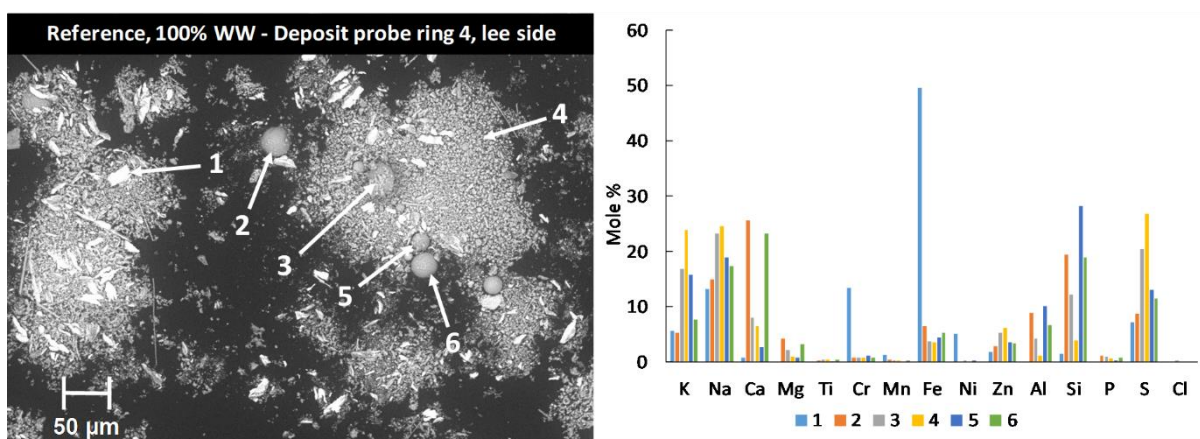


Figure 46. Example of the composition of different particles in the sample from the deposit probe ring, lee side, from the reference run. Here, the Fe and Cr rich, light particles, (nr 1) probably has originated from the probe rings.

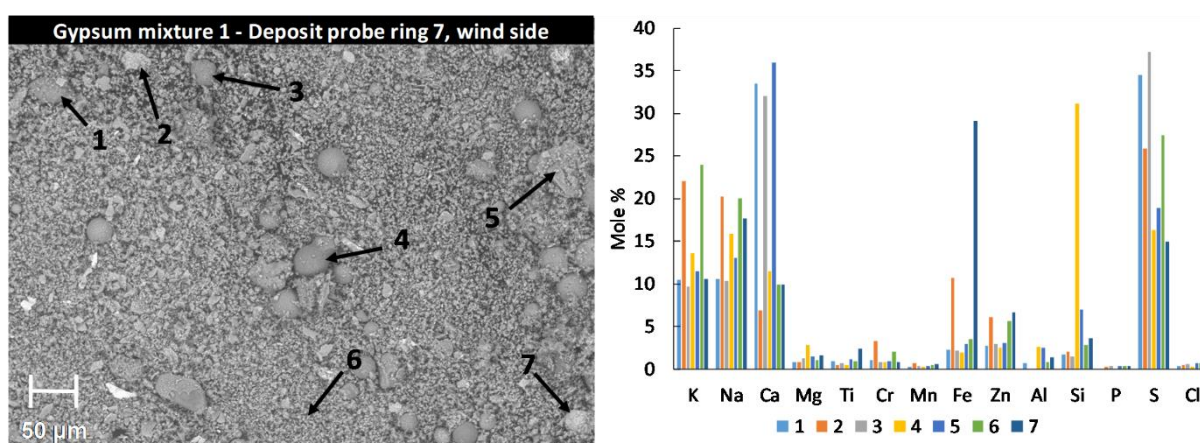


Figure 47. Example of the composition of different particles in the sample from the deposit probe ring, wind side, from the run with gypsum mixture 1.

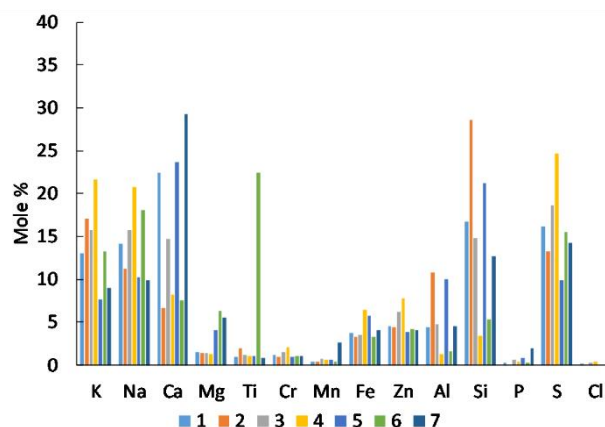
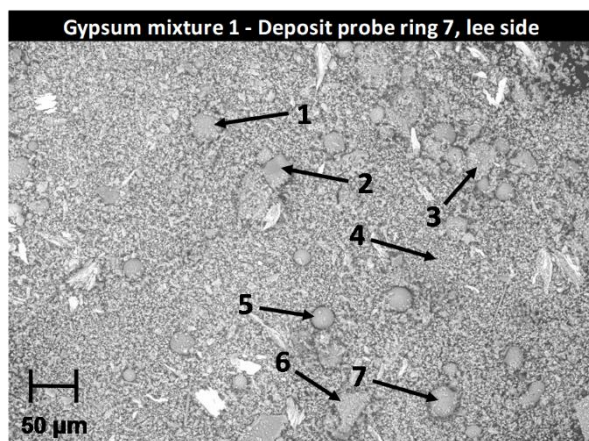


Figure 48. Example of the composition of different particles in the sample from the deposit probe ring, lee side, from the run with gypsum mixture 1.

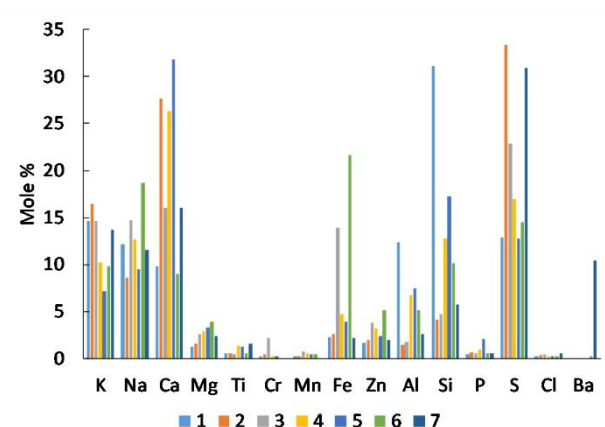
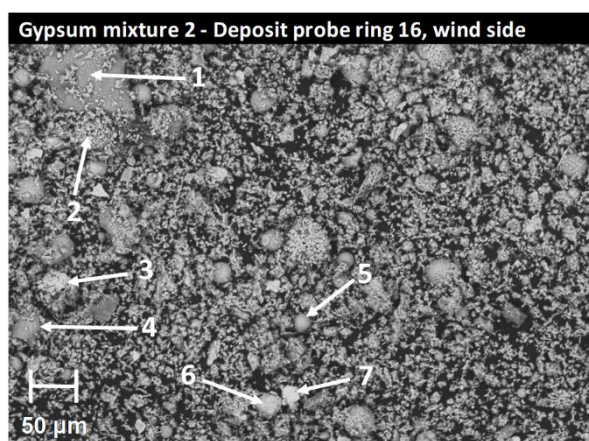


Figure 49. Example of the composition of different particles in the sample from the deposit probe ring, wind side, from the run with gypsum mixture 2.

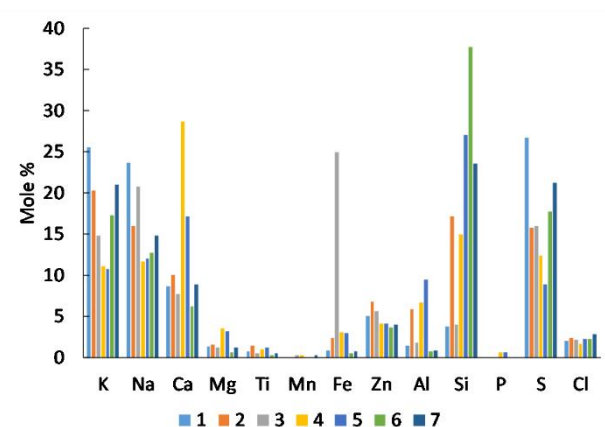
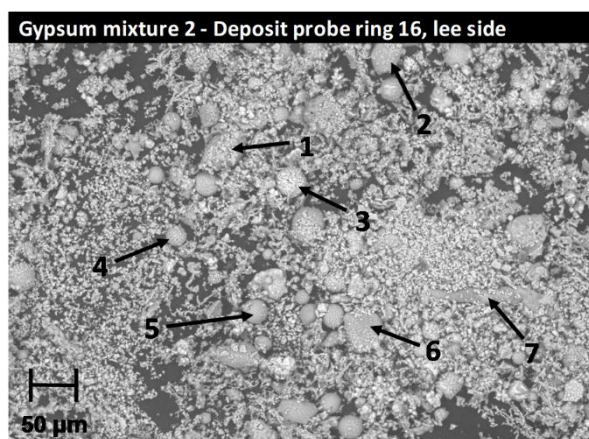


Figure 50. Example of the composition of different particles in the sample from the deposit probe ring, lee side, from the run with gypsum mixture 2.

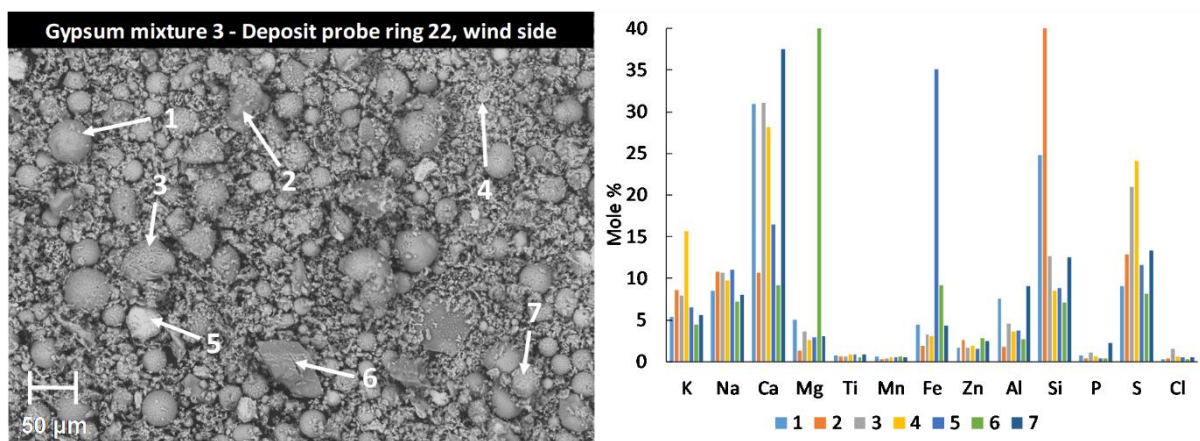


Figure 51. Example of the composition of different particles in the sample from the deposit probe ring, wind side, from the run with gypsum mixture 3.

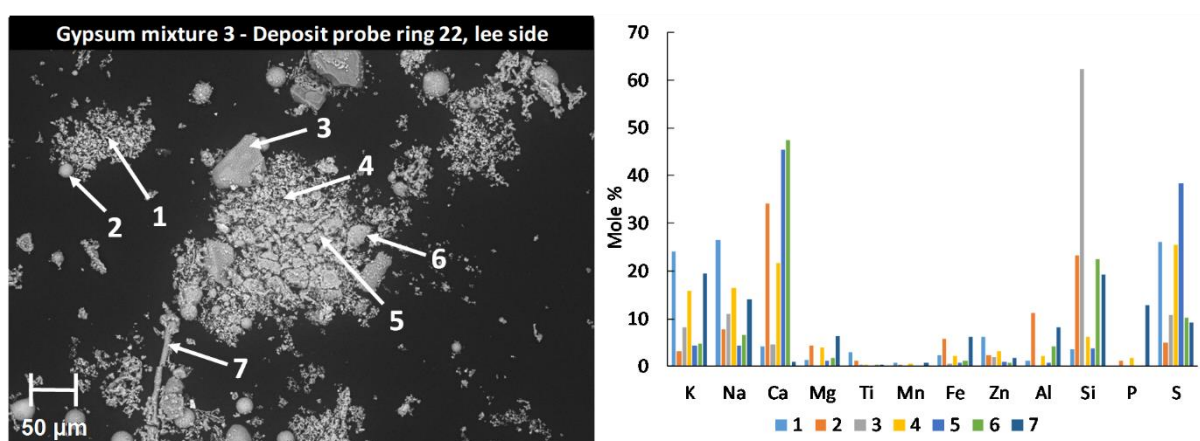


Figure 52. Example of the composition of different particles in the sample from the deposit probe ring, lee side, from the run with gypsum mixture 3.

3.3.4.3 PXRD-analysis

Deposit probe – lee-side

The small amounts of sample only allowed for compound identification and not quantification for these cases. Only samples G1 and G2 yielded diffractograms of good quality as the other samples displayed very low intensities. However, in these cases the presence of mixed sulphates was interesting. The presence of mixed K-Ca-sulphates indicate that even if the gypsum particles are entrained, they may still interact with gaseous alkali-containing compounds. The reference case may contain trace amounts of the mixed K-Na-sulphate aphtitalite.

Table 9. Crystalline compounds identified in deposition probe lee-side from industrial-scale experiments. The amounts of asterisks represent how dominant the respective phase is based on relative peak height. *) Observed; **) Minor, ***) Major.

Formula	Trivial name	Reference	G1	G2	G3
CaSO ₄	Anhydrite		**	**	*
K ₂ Ca ₂ (SO ₄) ₃				**	
K ₃ Na(SO ₄) ₂	Aphtitalite	*	***	***	
KCl	Sylvite			**	
ZnO	Zincite			*	

Deposit probe – wind-side

The small amounts of sample only allowed for compound identification in some of these deposit probe wind-side samples. Again there mixed K-Ca-sulphates is present in the additive cases which further emphasises that these compounds likely are important, although it cannot be certainly determined if this is caused by alkali reacting directly with gypsum particles or if they are discrete alkali sulphates particles adhering to gypsum that react over time. Pure calcium sulphate is also identified for all cases which shows that even in the reference case, there is a significant sulphation potential. Interestingly, no chlorides were positively identified.

Table 10. Crystalline sulphate compounds identified in deposition probe wind-side from industrial-scale experiments. The amounts of asterisks represent how dominant the respective phase is based on relative peak height. *) Observed; **) Minor, ***) Major.

Formula	Trivial name	Reference	G1	G2	G3
CaSO ₄	Anhydrite	**	**	**	***
K ₂ Ca ₂ (SO ₄) ₃			*	***	**
K ₃ Na(SO ₄) ₂	Aphtitalite	**	***	**	**

3.4 Discussion and conclusions

The demonstration of gypsum as a simultaneous additive providing CaO and SO_{2/3} has yielded mixed results. From the chemical point of view, the flue gas analysis clearly shows that the gypsum particles are dehydrated and later decomposes to release gaseous SO_x as shown by the elevated SO₂ levels detected for all cases of gypsum addition. HCl(g) are doubled in all cases of gypsum addition which further demonstrates that significant amounts of Cl are removed from solid deposits to be found in flue gases instead. There is clear evidence of K capture in particles with Ca and in bottom ash particles, as well as similar indications in the entrained fly ashes. The identification of mixed K-Ca-sulphates in deposit samples are important, since deposits and fouling may cause alkali-induced corrosion. Even though little to no Cl was present even for the reference case this may prove important for more challenging fuels than the relatively clean reference fuel used in this work.

Fuel blending seemingly worked well for the three different strategies. A potential effect of employing an Alu-blender could be the larger amounts of deposit formation observed. It could not be concluded whether the increased deposits were caused by smaller additive particles, increased amounts of small fuel particles, or a combination of both.

The actual effect on operational parameters is more difficult to conclude from the results obtained here, however. There were little to no slagging indications for the reference case, and consequently, the only indication of whether gypsum is a potential additive is the absence of increased slag formation. Total particulate matter amounts increased and so did deposit formation, but deposits were not rich in Cl and therefore not as likely to cause elevated risks of high-temperature corrosion. The increased SO_x and HCl concentrations in flue gases were readily managed by existing installations to maintain the plant within its environmental permit.

The demolition wood used in this full-scale trial had an ash composition with only low or moderate levels of the potentially problematic elements K, Na, Zn, and Cl. Based on the above observations, this may not be the type of demolition wood that gypsum would be the most suitable additive for. In cases where there are operational issues with slagging or chloride-induced high-temperature corrosion during normal operation, gypsum could likely offer alleviation in industrial scale. This would place some prerequisites on possibility remove particulate matter and clean flue gases which are typically present at plants allowed to combust waste streams such as demolition wood.

3.4.1 Conclusions

Gypsum as an additive for simultaneous addition of Ca and S to problematic waste streams still shows potential. This results here show that the underlying chemical reactions work as intended, but the demolition wood used for co-combustion did not produce slag or chloride-rich deposits without the additive.

- Fuel admixing worked similarly well regardless of strategy, but the additive dosing system needs to be adjusted to different fuel feeding systems and to each specific combustion system.
- Fuel composition was inherently non-problematic from a slagging perspective so effect of Ca from gypsum on slagging issues could not be conclusively evaluated
- Alkali capture in mixed Ca-sulphate particles was readily observed which indicates good potential to reduce chloride formation
- Increased flue gas concentrations of HCl in combination with elevated SO₂ concentrations shows a reduction of chloride formation
- Gypsum addition should primarily be considered for fuels that will benefit greatly from additional Ca and S in the fuel blend
- Power plant capabilities for handling of total particulate matter concentrations in cyclone or filters as well as flue gas cleaning must be considered if gypsum is used as an additive



RISE Research Institute of Sweden
Box 857, 501 15 Borås, Sweden
Phone: 010-516 50 00
Email: info@ri.se, Internet: www.ri.se

Report :Final
REFAWOOD report for
WP3